Schubert Geometry of Flag Varieties and Gelfand-Cetlin Theory

by

Mikhail Kogan

Bachelor of Arts, New York University, June 1995

Submitted to the Department of Mathematics
in partial fulfillment of the requirements for the degree of

Doctor of Philosophy

at the

MASSACHUSETTS INSTITUTE OF TECHNOLOGY

June 2000

Signature redacted

Author .....
Department of Mathematics
May 3, 2000

Signature redacted

Certified by .....
Victor Guillemin
Professor of Mathematics
Thesis Supervisor

Signature redacted

Accepted by .....
Tomasz S. Mrowka
Chairman, Departmental Committee on Graduate Students

Schubert Geometry of Flag Varieties and Gelfand-Cetlin Theory

by

Mikhail Kogan

Submitted to the Department of Mathematics
on May 3, 2000, in partial fulfillment of the
requirements for the degree of
Doctor of Philosophy

Abstract

This thesis investigates the connection between the geometry of Schubert varieties and Gelfand-Cetlin coordinates on flag manifolds. In particular, we discovered a connection between Schubert calculus and combinatorics of the Gelfand-Cetlin polytope.

In [13] Guillemin and Sternberg constructed a set of action coordinates on a flag manifold, which maps this flag manifold to the Gelfand-Cetlin polytope. We show that every Schubert cycle is equivariantly cohomologous to a canonical linear combination of preimages of faces of the Gelfand-Cetlin polytope.

These faces can be identified with RC-graphs, which play a crucial role in the theory of Schubert polynomials. Using RC-graphs, we give a generalized Littlewood-Richardson rule, which provides an algorithm for multiplying certain Schubert polynomials by Schur polynomials.

Thesis Supervisor: Victor Guillemin
Title: Professor of Mathematics

Acknowledgments

A lot of people helped me on my way to writing this thesis. I would like to start with thanking my High School teachers S. E. Rukshin and V. A. Ryzik, who led me through my first steps in Mathematics.

I am greatly indebted to Professor Cappell for his generous help during my first year in the United States, as well as Professors Cheeger and Bogomolov who taught me a lot during my undergraduate studied at NYU.

I am extremely grateful to my advisor Victor Guillemin. It was a great privilege for me to work with him. Without his guidance, help and encouragement this thesis would not be possible.

It is a pleasure to thank Allen Knutson and Sara Billey for many very useful discussions and suggestions. In particular, I am grateful to Allen for his suggestion to think about the images of Schubert varieties under the Gelfand-Cetlin map and to Sara for recognizing RC-graphs in the reduced faces of the Gelfand-Cetlin polytope.

I thank Edik Goldstein, Sasha Soloviev and Sasha Perlin for being very good friends during my long 5 years at MIT.

I'd like to express deep gratitude to my parents for their constant support. To them I owe most of what I have achieved in life.

Finally, let me thank my wife Tanya, who never stopped believing in me. I dedicate this thesis to her.

Contents

Chapter 1

Introduction

The main goal of this thesis is to understand the connection between the classical theory of Schubert varieties and the less studied theory of Gelfand-Cetlin action coordinates. The thesis contains two almost independent parts. The first part constructs new cycles for Schubert varieties using faces of the Gelfand-Cetlin polytope and the second part describes a generalized Littlewood-Richardson rule for multiplying Schur polynomials by Schubert polynomials. This rule involves the theory of RC-graphs, which are generalizations of Young tableaux and turn out to be closely related to the Gelfand-Cetlin polytope.

1.1 Schubert varieties and Gelfand-Cetlin theory

In [13] Guillemin and Sternberg defined a set of action coordinates on each flag manifold. Given a weight λ of $SU(n)$, these coordinates give a "moment" map Φ on the manifold of complete flags Fl_n, which takes Fl_n onto the classical Gelfand-Cetlin polytope. (This polytope was originally introduced in [10]. Lattice points inside the polytope give a canonical basis of the irreducible representation of $SU(n)$ with the highest weight λ.) Roughly speaking, the set of these action coordinates is a classical mechanic analogue of the Gelfand-Cetlin basis in quantum mechanics. Since we can think of a set of action coordinates as a solution to a classical mechanical system, it is natural to assume that we can learn a lot about Fl_n just by looking at these coordinates.

In the second chapter we try to show how most of the information about the Schubert calculus can be extracted from the combinatorics of the Gelfand-Cetlin polytope.

Let us recall a few facts about Schubert varieties. For each permutation $w \in S_n$ we

can define a subvariety $X_w \in Fl_n$, called a Schubert variety. The cohomology classes $[X_w]$ defined by Schubert varieties form a basis for the cohomology of Fl_n. Moreover, if we consider the standard $n-1$ torus T action on Fl_n, each Schubert variety defines an equivariant cohomology class and they generate $H_T^*(Fl_n)$ as a $S(\mathfrak{t}^*)$ module ($S(\mathfrak{t}^*)$ is the algebra of the polynomials on the dual $\mathfrak{t}^*$ of the Lie algebra of T.)

In Section 2.2 we will define a set of *reduced faces* of the Gelfand-Cetlin polytope and for each reduced face D define a permutation $w(D)$. (These faces can be identified with an already known combinatorial object called RC-graphs.) It turns out that all the information about the equivariant cohomology classes of the Schubert varieties is contained in these reduced faces. We will prove the following three theorems, which link the Schubert calculus to the combinatorics of the Gelfand-Cetlin polytope.

The first theorem says which Schubert varieties map to faces of the Gelfand-Cetlin polytope under the map Φ and hence have a set of action coordinates themselves. Proposition 2.3.2 also shows that these Schubert varieties are actually Kempf varieties, which were algebraically degenerated to toric variety by Gonciulea and Lakshmibai in [12].

Theorem 2.3.1 *If, for a permutation w, there is a unique reduced face D with $w(D) = w$ then $\Phi^{-1}(D) = X_w$.*

The second theorem shows that each equivariant cohomology class defined by a Schubert variety is given by an equivariant cycle, defined by taking preimages of certain prescribed reduced faces of the Gelfand-Cetlin polytope.

Theorem 2.4.1 *For a permutation $w \in S_n$, let*

$$W_w = \Phi^{-1}(\bigcup_{w(D)=w} D).$$

Then W_w defines an equivariant cohomology class $[W_w] \in H_T^*(Fl_n)$ and

$$[X_w] = [W_w].$$

The third theorem shows that double Schubert polynomials P_w can be written explicitly in terms of the combinatorial information about the reduced faces of the Gelfand-Cetlin

polytope. We will define P_w as well as polynomials P_D for each reduced face D in Section 2.5.

Theorem 2.5.1 *For a permutation w, P_w is equal to the sum of P_D with $w(D) = w$, that is*

$$P_w = \sum_{w(D)=w} P_D.$$

The organization of the second chapter is the following. In section 2.1 we fix notations and recall basic definitions. Section 2.2 deals with combinatorics of the faces of the Gelfand-Cetlin polytope. In particular, we define reduced faces and their corresponding permutations. Section 2.3 proves Theorem 2.3.1, while Section 2.4 proves our main result: Theorem 2.4.1. The proof of this theorem contains two major parts. The first part shows that the equivariant cohomology class $[W_w]$ is well defined using the technical Lemma 2.4.2. The second part proves that $[X_w] = [W_w]$ using Kirwan injectivity theorem. In Section 2.5 we present Theorem 2.5.1 and show that it is essentially equivalent to a result proved by Fomin and Kirillov in [7]. Section 2.6 gives another example of equivariant cohomology classes, which can be realized using preimages of faces of the Gelfand-Cetlin polytope. Finally, in the Appendix, we define equivariant cohomology using currents and prove that this definition coincides with the standard definition of equivariant cohomology. (We need this to define equivariant cohomology classes given by preimages of the faces of the Gelfand-Cetlin polytope.)

1.2 RC-graphs and Littlewood-Richardson rule

In the third chapter we provide a "Littlewood-Richardson" rule for multiplying certain Schubert polynomials by Schur polynomials. It turns out that we can think of Young tableaux as being special RC-graphs (which are also reduced faces of the Gelfand-Cetlin polytope). This leads to a straightforward generalization of the Schensted algorithm (see [1]). In the special case, considered by us in this thesis, this algorithm preserves some of the key properties of the classical Schensted algorithm for Schur polynomials. (This allows us to prove a more general Littlewood-Richardson rule than was previously known.)

We will denote by w a permutation, which permutes all integers, which are not greater than n, such that there exists N with $w(i) = i$ for every $i \leq -N$. Moreover, we will always

assume that w possesses the following property:

$$w(i) > w(i-1) \text{ if } i \leq 0.$$

Let $\mu = (\mu_1, ..., \mu_n)$ be a partition with $\mu_1 \geq ... \geq \mu_n$. Then we can associate to each partition a permutation $w(\mu)$, which will be defined in Section 3.1. Let S_w be the Schubert polynomial of w and let $S_\mu = S_{w(\mu)}$ be the Schur polynomial of μ. Since Schubert polynomials form a basis for the ring of all polynomials, we can write

$$S_w S_\mu = \sum_u c^u_{w,\mu} S_u,$$

where the sum is taken over all permutations u. The coefficients $c^u_{w,\mu}$ are known to be positive and are called the generalized Littlewood-Richardson coefficients. Our goal is to provide a rule for computing these coefficients.

An RC-graph R will be a collection of tuples $\{(i,k) | i,k \leq n\}$, which satisfy some additional properties. Graphically an RC-graph represents a planar history of the permutation w_R (again, we always assume w_R satisfies the property that $w(i) > w(i-1)$ if $i \leq 0$). Each RC-graph can be thought of as a table of intersecting and nonintersecting strands, such that no two strands intersect more than once. The details are provided in Section 3.1.

Define x^R to be the product of all x_k's, with one x_k for each $(i,k) \in R$. Then we have

$$S_w = \sum_{w_R = w} x^R.$$

Moreover to each Young tableaux Y of shape $\mu(Y)$ we can associate a unique RC-graph $R(Y)$, which satisfies $w_{R(Y)} = w(\mu(Y))$ and

$$S_\mu = \sum_{\mu(Y)=\mu} x^Y = \sum_{\mu(Y)=\mu} x^{R(Y)}$$

This shows that RC-graphs are generalizations of Young tableaux and suggests that we can generalize a lot of properties of Young tableaux to RC-graphs.

In particular, Bergeron and Billey in [1] provided a generalization of the Schensted insertion algorithm to the case of RC-graphs. We describe this algorithm for the special Schubert polynomials considered here in Section 3.2. We denote by $R \leftarrow k$ the result of

the insertion of a number $1 \leq k \leq n$ into an RC-graph R, and by $R \leftarrow Y$, the result of the insertion of a Young tableau Y into an RC-graph R.

The key fact, which makes the generalized Littlewood-Richardson rule possible to prove is the following lemma, which generalizes the row bumping lemma (see [9]) in the case of the classical Schensted algorithm. We will give precise definitions of the paths of insertions in Section 3.3. Roughly speaking these paths are the parts of RC-graphs, which are changed during the insertion algorithms. Let us emphasize the fact that the following lemma does not hold for the general insertion algorithm of Billey and Bergeron, but works only in the special case we consider.

Lemma 3.2.2 *If $x \leq y$, then the path of x is weakly to the left of the path of y in $R \leftarrow xy$. If $x > y$ then the path of x is weakly to the right of the path of y in $R \leftarrow xy$.*

This lemma plays a pivotal role in the proof of the following theorem which describes the Littlewood-Richardson rule mentioned above.

Theorem 3.3.1 *Let w be a permutation, which satisfies $w(i) > w(i-1)$ for each $i \leq 0$ and let μ be any partition. Choose any RC-graph U and set $w_U = u$. Then $c^u_{w,\mu}$ is equal to the number of pairs (R, Y) of an RC-graph R and a Young tableau Y with $w(R) = w$ and $\mu(Y) = \mu$, such that $R \leftarrow Y = U$.*

The proof of this theorem consists of three major steps. The first step is to prove the theorem for the simplest partitions ν_m, which are just given by one number m. The second step is to show that all other Schur polynomials can be expresses in terms of the simplest Schur polynomials S_{μ_m}. And finally, the third step is to prove $(R \leftarrow Y_1) \leftarrow Y_2 = R \leftarrow (Y_1 \leftarrow Y_2)$. The theorem follows easily from these facts.

The organization of the third chapter is as follows. In Section 3.1 we recall basic definitions and properties of RC-graphs and Young tableaux. Section 3.2 describes the insertion algorithm together with the proof of Lemma 3.2.2, and section 3.3 proves Theorem 3.3.1 using the three facts mentioned above. Finally Section 3.4 proves these three technical facts.

Chapter 2

Equivariant Cohomology Classes of Schubert Varieties and Gelfand-Cetlin Action Coordinates

2.1 Preliminaries

2.1.1 Flag manifolds

Let $G = SU(n)$ with a Cartan subtorus T. Let $\mathfrak{g}$, $\mathfrak{t}$ be their Lie algebras and let $\mathfrak{g}^*$, $\mathfrak{t}^*$ be the corresponding duals. We can identify $\mathfrak{g}^*$ with $n \times n$ traceless Hermitian matrices, while $\mathfrak{t}$, which consists of diagonal matrices with $(x_n, ..., x_1)$ on the diagonal and with $\sum_i x_i = 0$, gets identified with $\mathbb{R}^{n-1}$. Choose a positive Weyl chamber $\mathfrak{t}^*_+$ inside $\mathfrak{t}^*$ such that simple roots are given by $x_{i+1} - x_i \in \mathfrak{t}^*$. For $\lambda \in \mathrm{int}(\mathfrak{t}^*_+)$ let O_λ be the coadjoint orbit which passes through λ.

We will think of O_λ as the set of $n \times n$ traceless Hermitian matrices with fixed eigenvalues given by $\lambda = (\lambda_1, ..., \lambda_n)$ with $\lambda_1 < ... < \lambda_n$. If $A \in O_\lambda$ and $v_1, ..., v_n$ are the respective eigenvectors of the matrix A then the vector spaces V_i spanned by $v_1, .., v_i$ form a complete flag in $\mathbb{C}^n$. This identifies O_λ with the flag manifold Fl_n.

The Weyl group of G is generated by simple reflections s_i given by sending x_{i+1} to x_i and x_i to x_{i+1}. It can be identified with the group S_n of permutations of n elements. When no confusion may arise we will also denote by s_i a simple transposition, which permutes elements i and $i+1$ when acted on a right of a permutation w, that is $ws_i(i) = w(i +$

1) and $ws_i(i+1) = w(i)$. $s_1, ..., s_{n-1}$ generate S_n. The composition $w = s_{i_1}...s_{i_k}$ is a *reduced expression* of w if there is no way of writing w as a product of less than k simple transpositions. The length of w is then equal to k and is denoted by $l(w)$. The longest permutation w_0 has length $\frac{n(n-1)}{2}$ and satisfies $w_0(i) = n-i+1$. We say that a permutation w is greater than w' *with respect to the Bruhat order* if there exist a reduced expression $w = s_{i_1}...s_{i_k}$ such that by deleting some simple transpositions from it we get a reduced expression for w'.

For a permutation w we define the *Schubert variety* $X_w \subset Fl_n$ as the set of all flags $V = (V_1, ..., V_n)$ in $\mathbb{C}^n$ which satisfy $\dim(V_i \cap F_j) \geq \#\{k \leq i, w(k) > n-j\}$ for all i, j ($(F_1, ..., F_n)$ is the flag given by the diagonal matrix $(\lambda_n, ..., \lambda_1)$.) A result of Chevalley (see [5]) states that $w \leq w'$ with respect to the Bruhat order if and only if $X_{w'} \subset X_w$.

The Cartan subgroup of G, the $n-1$ dimensional torus T, acts on Fl_n in a Hamiltonian fashion. Denote by $\phi : FL_n \to \mathfrak{t}^*$ a moment map of this action. We can choose ϕ to be just the composition of the inclusion $O_\lambda \to \mathfrak{g}^*$ and the projection $\mathfrak{g}^* \to \mathfrak{t}^*$. More explicitly, $\phi(A)$ is given by taking the diagonal elements of a Hermitian matrix A. The image of ϕ is a convex polytope which is invariant with respect to the Weyl group $W = S_n$ action.

The fixed point set of the T action on Fl_n is given by the preimages of the vertices of the polytope $\phi(Fl_n)$. These vertices form a Weyl group orbit $W \circ (\lambda_n, ..., \lambda_1)$. To a fixed point p we associate a permutation w_p, such that $\phi(p) = w_p(\lambda_n, ..., \lambda_1) = (\lambda_{w_p(n)}, ..., \lambda_{w_p(1)})$. This identifies the set of the fixed points of the T action with the Weyl group S_n.

Let us describe the weights of the T action on the tangent space T_pFl_n for each fixed point p. If w_p is just the identity element of S_n, then this set of weights is just the set of all negative roots $\Delta_- = \{x_i - x_j | i < j\}$. For general p, the set of weights of the T action on T_pFl_n is given by $w_p\Delta_- = \{x_{w_p^{-1}(i)} - x_{w_p^{-1}(j)} | i < j\}$.

2.1.2 Gelfand-Cetlin action coordinates on flag manifolds

The *Gelfand-Cetlin action coordinates* on Fl_n, which originally appeared in [13], are defined as follows. For a Hermitian $n \times n$ matrix A with eigenvalues $\lambda_1, ..., \lambda_n$, consider a $(n-k) \times (n-k)$ submatrix A_k consisting of the intersection of the first $n-k$ rows and the first $n-k$ columns. Denote by $\lambda_{k+1,k} \leq ... \leq \lambda_{n,k}$ the eigenvalues of A_k, where $\lambda_{i,0} = \lambda_i$. The collection of all of these functions for all k forms a set of Gelfand-Cetlin coordinates on Fl_n. These functions satisfy the following inequalities which come from the classical minimax

principle:

$$\lambda_{i,k} \leq \lambda_{i+1,k+1} \leq \lambda_{i+1,k}.$$

These inequalities define the Gelfand-Cetlin polytope in $\mathbb{R}^{\frac{n(n-1)}{2}}$.

Moreover, if we denote by Φ the map which takes Fl_n to $\mathbb{R}^{\frac{n(n-1)}{2}}$, then $\Phi(Fl_n)$ is the whole Gelfand-Cetlin polytope and Φ provides a set of *action* coordinates on Fl_n (with respect to the Kirillov-Kostant symplectic form on O_λ). In other words, the functions $\lambda_{i,k}$ form a set of commuting independent Hamiltonians, whose flows, where defined, are periodic. Notice that the function $\lambda_{i,k}$ is not smooth if and only if $\lambda_{i,k} = \lambda_{i+1,k}$ or $\lambda_{i,k} = \lambda_{i-1,k}$. So, if we define an open dense set U in Fl_n to be the set of all Hermitian matrices with $\lambda_{i,k} \neq \lambda_{i+1,k}$ for every i, k, then $\Phi|_U$ is a moment map of a $\frac{n(n-1)}{2}$ dimensional torus action on U.

The action of the Cartan subtorus T on Fl_n is a subaction of the $\frac{n(n-1)}{2}$ dimensional torus action on U mentioned above. So that, if P is the natural projection from the Gelfand-Cetlin polytope to $\mathfrak{t}^*$, then $\phi = P \circ \Phi$. This projection P is given by:

$$P(\lambda_{i,k}) = (\lambda_{n,n-1}, \sum_i \lambda_{i,n-2} - \lambda_{n,n-1}, \ldots, \sum_i \lambda_{i,1} - \sum_i \lambda_{i,2}, \sum_i \lambda_{i,0} - \sum_i \lambda_{i,1})$$

or, in other words, the coordinate x_k of the moment map ϕ is given by $\sum_i \lambda_{i,k-1} - \sum_i \lambda_{i,k}$. For more details about Gelfand-Cetlin action coordinates see [13].

2.2 Combinatorics of the Gelfand-Cetlin polytope

It turns out that there is a strong connection between Schubert varieties and preimages of the faces of the Gelfand-Cetlin polytope. We devote this section to talking about the combinatorics of these faces.

2.2.1 Reduced Faces

It is easy to see that each face D of the Gelfand-Cetlin polytope is given by a set of equalities of types A and B:

$$\lambda_{i,k} = \lambda_{i+1,k+1} \quad (A_{i,k})$$

$$\lambda_{i,k} = \lambda_{i,k+1} \quad (B_{i,k})$$

Each face will be described by a triangular diagram (denoted by the same letter D) which will consist of these equalities. To explain better what we mean by these diagrams we provide the following examples.

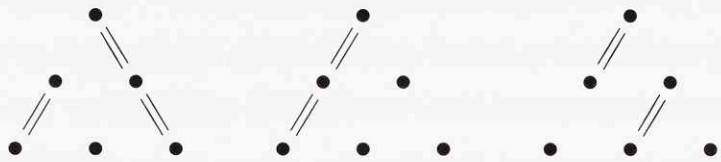

Figure 1: Examples of faces of the Gelfand-Cetlin polytope.

In Figure 1, $n = 3$, the first diagram is the face given by the equalities $A_{1,0}, B_{3,0}$ and $B_{3,1}$ (in other words: $\lambda_1 = \lambda_{2,1}$ and $\lambda_3 = \lambda_{3,1} = \lambda_{3,2}$). The second face is defined by $A_{1,0}$ and $A_{2,1}$ ($\lambda_1 = \lambda_{2,1} = \lambda_{3,2}$). Finally, the last diagram is defined by $A_{2,1}$ and $A_{2,0}$ ($\lambda_{2,1} = \lambda_{3,2}$ and $\lambda_2 = \lambda_{3,1}$).

A word of warning is in place. Not all these equalities are independent. For example, if the equalities $A_{i,k}$ and $B_{i+1,k}$ hold then they force both $A_{i,k-1}$ and $B_{i,k-1}$ to hold. So, we will always assume that all the equalities for the given face are included in the triangular diagrams. For example, in Figure 2 all diagrams define the same face, but we will only use the third diagram when we talk about this face.

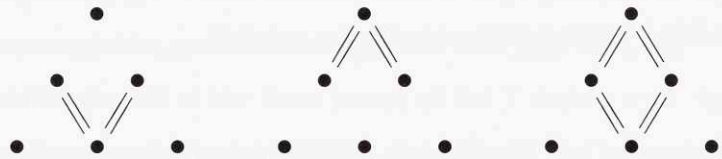

Figure 2: These diagrams define the same face in the Gelfand-Cetlin polytope.

We will be mainly interested in the faces given only by the equalities of type $A_{i,k}$. For each such face D we define a permutations $w(D)$ in the following way. Each equality $A_{i,k}$ will produce a simple transposition s_i. To define $w(D)$ we compose these simple transpositions by going from right to left in each row of the diagram D and by going from the bottom row to the top one. We will be interested only in those faces for which the expressions for the permutation $w(D)$ given by our diagrams are reduced. We call these faces *reduced*.

For example, Figure 1 contains two diagrams with no $B_{i,k}$'s in them. These are the second and third diagrams. But only the second diagram is reduced, since w(third diagram) $= s_2 s_2 =$id, while w(second diagram) $= s_1 s_2 = (231)$.

The reduced faces of the Gelfand-Cetlin polytope have been studied before. They turn

out to be equivalent to the RC-graphs, which were introduced by Fomin and Kirillov in [7] and were later studied by Bergeron and Billey in [1]. (Indeed, if we substitute each equality $A_{i,k}$ in D by intersecting strands, and all the equalities $A_{i,k}$ not in D by nonintersecting strands and then connect the strands, we will get an RC-graph.)

We will not attempt to give here a detailed discussion of RC-graphs and postpone it until Chapter 3, but will recall some basic facts about them and translate these facts into the language of the Gelfand-Cetlin polytope.

- Let D be a reduced face, such that $A_{i,k}, A_{i+1,k}$ and $A_{i+\ell+1,k+\ell}$ are not in D for some i, k and ℓ, but all other $A_{i',k'}$ with $k \leq k' \leq k+\ell$ and $0 \leq (i'-k') - (i-k) \leq 1$ are in D. Then we can substitute $A_{i+\ell,k+\ell}$ by $A_{i+1,k}$ without changing $w(D)$. (We also can go backwards.) These operations are called *ladder moves* of size ℓ at the place (i,k). Examples of ladder moves of sizes 1 and 2 are shown on Figure 3.

- For every permutation w there exist a unique reduced diagram D_w (which we will call the *Gelfand-Cetlin diagram* of w), such that every other reduced diagram D with $w(D) = w$ can be constructed from D_w by a sequence of ladder moves, which substitute $A_{i+\ell,k+\ell}$ by $A_{i+1,k}$ (but not the other way).

- Each Gelfand-Cetlin diagram D_w satisfies the following property. If an equality $A_{i,k}$ is a part of it and $i \geq k+1$, then $A_{i-1,k}$ is also a part of D_w. In other words, the equalities $A_{i,k}$ are concentrated strictly to the left in each row of D_w.

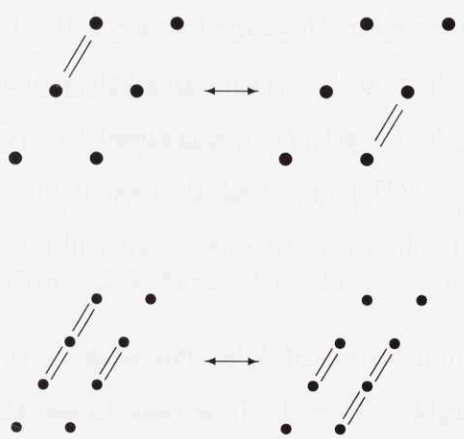

Figure 3: Examples of ladder moves of sizes 1 and 2.

We need to describe all the permutations w for which there is a unique face D with

$w(D) = w$. It is easy to see that each Gelfand-Cetlin face D_w produces a reduced expression of $w(D)$ of the form $u_1 ... u_{n-1}$ with $u_k = s_{j_k} s_{j_k+1} ... s_{k-1} s_k$.

Proposition 2.2.1 *A permutation w has a unique face D with $w(D) = w$ if and only if $j_k + 1 \geq j_{k+1}$ for every k.*

Proof. Look at the Gelfand-Cetlin diagram D_w of w. It is clear that it is impossible to apply any ladder moves to it if and only if $j_k + 1 \geq j_{k+1}$ for every k. Hence proposition holds. □

2.2.2 Nondegenerate Vertices

Another type of face we are going to be interested in is a vertex (face of dimension zero) of the Gelfand-Cetlin polytope for which $\lambda_{i,k} \neq \lambda_{i+1,k}$ for every i, k. In other words, each such vertex is an image of some fixed point $p \in Fl_n^T$. The diagram D, which defines such a vertex has the following property:

- Each row k of D contains exactly $n - k - 1$ equalities and $A_{i,k}$'s are strictly to the left of $B_{i',k}$'s.

These vertices will be called *nondegenerate vertices* of the Gelfand-Cetlin polytope. (We call them nondegenerate vertices, since these are exactly the simple vertices of the Gelfand-Cetlin polytope, i.e. vertices with precisely $\frac{n(n-1)}{2}$ edges coming out of them.) For example, the first diagram in Figure 1 is a nondegenerate vertex.

For each nondegenerate vertex p (which is denoted by the same letter p as the fixed point of the T action it corresponds to) we define the diagram D_p to contain all the equalities $A_{i,k}$ from the diagram which defines p but none $B_{i,k}$'s. Clearly D_p is a reduced face (moreover, it is even a Gelfand-Cetlin face), so we set $w_p = w(D_p)$. To check that the definition of w_p coincided with the geometric definition given in the previous section we will give another combinatorial definition of w_p.

Since p is a vertex, each $\lambda_{i,k}$ has to be equal to one of λ_j's. For each λ_j choose the largest k with $\lambda_{i,k} = \lambda_j$ for some i and set $w_p(k+1) = j$. It is easy to see that w_p is well-defined and the two combinatorial definitions of w_p are the same.

Let us now use the second combinatorial definition of w_p to show that it coincides with the geometric definition given in the previous section. We can think of the preimage $\Phi^{-1}(p)$

of a nondegenerate vertex p as of a diagonal matrix A given by by its diagonal elements $(\lambda_{i_n}, ..., \lambda_{i_1})$. We need to prove that $i_k = w_p(k)$. Recall that in the row $k-1$ of the diagram p, the unique eigenvalue which is not equal to any $\lambda_{i,k}$ is $\lambda_{i,k-1} = \lambda_{w_p(k)}$. But, since all the eigenvalues of A_{k-1} are the same as the eigenvalues of A_k, except for the eigenvalue $\lambda_{i,k-1} = \lambda_{w_p(k)}$, and A is diagonal, we can conclude that $\lambda_{i,k-1} = \lambda_{w_p(k)} = \lambda_{i_k}$ and hence $i_k = w_p(k)$. This shows that the three definitions of w_p are the same.

2.2.3 Edges coming out of the nondegenerate vertices

Let us describe all the edges, which come out of the nondegenerate vertices. The direction of these edges will determine the weights of the $\frac{n(n-1)}{2}$ dimensional torus action on T_pFl_n. It is not difficult to explicitly describe these weight, but we will be only interested in the projection of these edges onto $\mathfrak{t}^*$. In other words, we will need to know the weight of the T action on T_pFl_n.

There are exactly $\frac{n(n-1)}{2}$ edges coming out of each nondegenerate vertex, one edge for each equality $A_{i,k}$ or $B_{i,k}$ in the diagram of p. If we remove one equality $A_{i,k}$ (or $B_{i,k}$) from the diagram of p, we get an edge (a one-dimensional face of the Gelfand-Cetlin polytope) coming out of p, which we denote by $e_{i,k}$.

Recall that the projection P, takes the Gelfand-Cetlin polytope to $\mathfrak{t}^*$ by

$$P(\lambda_{i,k}) = (\lambda_{n,n-1}, \sum_i \lambda_{i,n-2} - \lambda_{n,n-1}, \ldots, \sum_i \lambda_{i,1} - \sum_i \lambda_{i,2}, \sum_i \lambda_{i,0} - \sum_i \lambda_{i,1})$$

Moreover, $P \circ \Phi$ is the moment map ϕ of the T action on Fl_n and takes Fl_n to $\mathfrak{t}^*$.

Fix a nondegenerate vertex p, set $w = w_p$. We are interested in the projections of the edges $P(e_{i,k})$ for each $A_{i,k}$ in the diagram of p. This projection will clearly be a ray coming out of the vertex $P(p)$ and pointing into the direction of the root $x_{\tilde{k}+1} - x_{k+1}$ of G, where $\tilde{k}$ is the largest possible row of the diagram of p with the property that $\lambda_{i,k} = \lambda_{j,\tilde{k}}$ for some j.

Proposition 2.2.2 *For each edge $e_{i,k}$ defined by removing $A_{i,k}$ from p, the root $x_{\tilde{k}+1} - x_{k+1}$ satisfies*

- $k < \tilde{k}$
- $w(k+1) > w(\tilde{k}+1)$.

In particular, all of the above roots form the set $\Delta_+ \cap w\Delta_-$.

Proof. The fact that $k < \tilde{k}$ is obvious. To prove the second property, find ℓ_1 which satisfies $\lambda_{\ell_1} = \lambda_{i,k} = \lambda_{j,\tilde{k}}$. Then $w(\tilde{k}+1) = \ell_1$. Let $\ell_2 = w(k+1)$ then there exists j' such that $\lambda_{\ell_2} = \lambda_{j',k}$, moreover, k is the largest possible with this property. This implies that neither $A_{j',k}$ nor $B_{j',k}$ are in the diagram of p, but since $A_{j,k}$ is in the diagram of p we conclude that $j' > j$. Hence $\lambda_{j',k} > \lambda_{j,k}$, which implies that $\lambda_{\ell_2} > \lambda_{\ell_1}$. Hence $\ell_2 > \ell_1$ and $w(k+1) > w(\tilde{k}+1)$.

Finally, recall that w takes $x_i - x_j$ into $x_{w^{-1}(i)} - x_{w^{-1}(j)}$. Hence the two properties of $x_{\tilde{k}+1} - x_{k+1}$ show that each such root is indeed in $\Delta_+ \cap w\Delta_-$. Since the number of roots in $\Delta_+ \cap w\Delta_-$ and the number of equalities $A_{i,k}$ in the diagram of p are the same and both equal to $\ell(w)$, we can easily conclude that $\Delta_+ \cap w\Delta_-$ and the set of roots $x_{\tilde{k}+1} - x_{k+1}$ defined by the edges with $A_{i,k}$ removed are the same. □

2.2.4 Fl_3 inside Fl_n

For each ladder move we are going to define an inclusion of Fl_3 into Fl_n. These inclusions will be used in the proof of Lemma 2.4.2.

Given a ladder move at the place (m,k) of size ℓ set $k_1 = k+\ell+2$, $k_2 = k+2$ and $k_3 = k+1$. Then we take all matrices $A \in O_\lambda$, which are diagonal outside the intersection of the rows k_1, k_2, k_3 and the columns k_1, k_2, k_3 of A (the rows of A are numbered starting with the bottom one, going to the top one, similarly the columns are numbered from right to left). Moreover, we specify the diagonal entries of A as follows. Starting at the top left corner and going to the bottom right corner of A, the diagonal entries should be $\lambda_1, ..., \lambda_{m-k-1}$ then $\lambda_{m+\ell+2}, ..., \lambda_n$ between the rows 1 and k_1, then $\lambda_{m+\ell+1}, ..., \lambda_{m+3}$ between the rows k_1 and k_2 and then $\lambda_{m-k}, ..., \lambda_{m+2}$ between the rows k_3 and n.

The set of all matrices A, which are described above form a three dimensional flag manifold Fl_3, which is embedded into Fl_n. Moreover, the image of this Fl_3 under the map Φ is given by the three-dimensional face $F_{m,k,\ell}$, which looks like the three dimensional Gelfand-Cetlin polytope and whose diagram can be defined as follows. $F_{m,k,\ell}$ contains all equalities of type A in each row above $k_1 - 1$. Below the row $k_3 - 1$, each row k' contains every $A_{i,k'}$ with $i \leq m+1$ and every $B_{i,k'}$ with $i \geq m+3$. Between the rows $k_1 - 1$ and $k_3 - 1$ each row k' contains every $A_{i,k'}$ with $i - k' \leq m - k + 1$ and every $B_{i,k'}$ with $i - k' \geq m - k + 3$. The row $k_1 - 1$ contains all equalities A_{i,k_1-1} with $i \leq m+\ell-1$ and all B_{i,k_1-1} with $i \geq m+\ell+2$. Finally, the row $k_3 - 1$ contains every A_{i,k_3-1} with $i \leq m-1$

and every B_{i,k_3-1} with $i \geq m+3$.

The reason we are interested in these faces of the Gelfand-Cetlin polytope is the following. Because of the very special choice of the embedding of Fl_3 into Fl_n, it is easy to understand how Φ behaves in the neighborhood of $\Phi^{-1}(F_{m,k,\ell}) = Fl_3$. More details will be given later, during the proof of Lemma 2.4.2.

2.3 Schubert varieties with action coordinates

The Gelfand-Cetlin action coordinates are defined on the flag manifold, so it is natural to ask whether they also provide action coordinates when restricted to the Schubert varieties. It turns out that it happens only for those Schubert varieties which map to faces of the Gelfand-Cetlin polytope. They are described in the following theorem.

Theorem 2.3.1 *If, for a permutation w, there is a unique reduced face D with $w(D) = w$ then $\Phi^{-1}(D) = X_w$.*

Proof. First of all, recall that by Proposition 2.2.1, if for a permutation w there is a unique face D with $w(D) = w$ then $w = u_1 ... u_{n-1}$ with $u_k = s_{j_k} s_{j_k+1} ... s_{k-1} s_k$ and $j_k + 1 \geq j_{k+1}$ for every k. Hence it is easy to see that X_w is the Schubert variety which contains only those flags $(V_1, ..., V_n)$ which satisfy

$$V_{j_k-k+1} \subset F_{n-k}. \tag{2.1}$$

This can be shown by induction. Let $w_i = u_1 ... u_i$. We will prove X_{w_i} is defined by the inclusions (2.1) for $k \leq i$. Clearly, X_{w_1} contains only those flags, which satisfy $V_{j_1} \subset F_{n-1}$. Moreover from $w_i u_{i+1} = w_{i+1}$, we know that $w_i < w_{i+1}$ and thus $X_{w_{i+1}} \subset X_{w_i}$. So, if (2.1) for $k \leq i$ holds for flags in X_{w_i}, it has to hold for flags in $X_{w_{i+1}}$. Moreover, flags in $X_{w_{i+1}}$ also have to satisfy $V_{j_{i+1}-i} \subset F_{n-i-1}$, since if $k \leq j_{i+1} - i$ then $w_{i+1}(k) > n - i - 1$ because of u_{i+1}. This proves that X_w is defined by the inclusions (2.1).

To prove the theorem we have to apply the classical minimax principle. Recall that if there is just one D with $w(D) = D$ then D is actually the Gelfand-Cetlin diagram of w, so that equalities in each row k are concentrated strictly on the left and there are exactly $j_k - k + 1$ of them. Let some Hermitian matrix A be in $\Phi^{-1}(D)$. The bottom row of the diagram D implies that j_1 smallest eigenvalues of A and A_1 coincide (where A_1 is the

$(n-1) \times (n-1)$ submatrix of A). Using minimax principle we can show that not only the smallest eigenvalues $\lambda_1, ..., \lambda_{j_1}$ but the corresponding eigenvectors $v_1, ..., v_{j_1}$ of these two matrices coincide as well. Hence we conclude that $V_{j_1} \subset F_{n-1}$, which is exactly the condition (2.1) for $k = 1$. Similarly, we know that the first $j_k - k + 1$ eigenvectors of the matrix A_k and A_{k-1} coincide, but using the fact that $j_k + 1 \geq j_{k+1}$ for each k, we conclude that the first $j_k - k + 1$ eigenvectors of A_k and A are the same. So, we can conclude that $V_{j_k-k+1} \subset F_{n-k}$. Hence every element in the preimage of the face is indeed in X_w.

Conversely, suppose we are given a Hermitian matrix A whose corresponding flag satisfies (2.1). Then $V_{j_k-k+1} \subset F_{n-k}$ implies that the smallest $j_k - k + 1$ eigenvalues of the matrices A_k and A_{k+1} coincide and again the minimax principle tells us that the corresponding eigenvalues should be the same. This proves that $\Phi(A) \in D$ and $\Phi(X_w) \subset D$, which finishes the proof of the Theorem. □

The permutations which appear in the above theorem have been studied by Lakshmibai in [18]. (This is the point of the next proposition. Since this proposition is not going to be used later, the reader can skip it if he so desires.)

Proposition 2.3.2 *If w is a permutation, which has a unique face D with $w(D) = w$, then it is a Kempf permutation and consequently X_w is a Kempf variety.*

Proof. We start by recalling one of Lakshmibai's definition of Kempf permutation given in [18]. She proves that every permutation w' could be written uniquely in the form $w_0 u'_1 ... u'_n$, where w_0 is the longest permutation and each u'_k is of the form $s_{i_k} ... s_{k+1} s_k$ for some i_k, $k \leq i_k \leq n$. Then $w' = w_0 u'_1 ... u'_n$ is Kempf if it satisfies $u'_k \leq u'_{k+1} s_k$ for every $1 \leq k \leq n$ or in other words $i_k \leq i_{k+1}$. (Actually, the index conventions in [18] are different from ours, so the definition of Kempf varieties in [18] looks different from the one above. We had to adopt Lakshmibai's definition to make conventions and notations fit.)

Recall that Proposition 2.2.1 shows that if w has a unique face D with $w(D) = w$, then $w = u_1 ... u_{n-1}$ with $u_k = s_{j_k} s_{j_k+1} ... s_{k-1} s_k$ and $j_k + 1 \geq j_{k+1}$ for every k.

We will prove by induction on n that if we have two permutations $w' = w_0 u'_1 ... u'_n$ and $w = u_1 ... u_{n-1}$ with $i_k + j_k = n - k$ then $w' = w$. If w' is Kempf and $i_k \leq i_{k+1}$ this will imply that $j_k + 1 \geq j_{k+1}$, which will prove the proposition.

For $n = 2$ the statement above is trivial. Let's assume we have proved this statement for $n - 1$ and we need to prove it for n.

We will prove that $(w')^{-1}w$ =id that is

$$(u'_n)^{-1}...(u'_1)^{-1}w_0u_1...u_{n-1} = \text{id}. \tag{2.2}$$

Actually, if $\tilde{w}_0$ is the longest permutation on the elements $2, .., n$, we will just have to prove that

$$(u'_1)^{-1}w_0u_1 = \tilde{w}_0, \tag{2.3}$$

and then apply the induction assumption to prove (2.2).

Using the fact that $s_iw_0 = w_0s_{n-i}$ we have:

$$(u'_1)^{-1}w_0u_1 = w_0s_{n-1}...s_{n-i_1}s_{j_1}...s_1 = w_0s_{n-1}...s_1 = \tilde{w}_0.$$

This proves (2.3) and finishes the proof of the proposition. □

Remark 2.3.3 Gonciulea and Lakshmibai in [12] showed how to algebraically degenerate each Kempf variety to a toric variety. Our approach produces a set of action coordinates on each Kempf variety by Theorem 2.3.1. We believe this is consistent with Gonciulea and Lakshmibai's result in the sense that these action coordinates should come from the moment map on the degenerated toric variety. But we do not have the precise proof of this.

2.4 Main theorem and its proof.

Unfortunately, most Schubert varieties do not map to faces of the Gelfand-Cetlin polytope. It is not clear what the image $\Phi(X_w)$ is in general, but we will show below that the equivariant cohomology class associated with X_w can be defined by a cycle consisting of preimages of faces of the Gelfand-Cetlin polytope.

The flag manifold Fl_n is equipped with a classical action of an $n-1$ torus (a Cartan subtorus T of $SU(n)$). It is clear that every Schubert variety as well as every preimage of a face of the Gelfand-Cetlin polytope is invariant under this action. Moreover, since every Schubert variety has algebraic singularities of codimension at least 2, it defines an equivariant cohomology class $[X_w] \in H^*_T(Fl_n)$.

Theorem 2.4.1 *For a permutation $w \in S_n$, let*

$$W_w = \Phi^{-1}(\bigcup_{w(D)=w} D).$$

Then W_w defines an equivariant cohomology class $[W_w] \in H_T^*(Fl_n)$ and

$$[X_w] = [W_w].$$

The rest of this section is concerned with the proof of this theorem. The first part of the proof will show that W_w indeed defines an equivariant cohomology class, while the second part will check that $[X_w] = [W_w]$.

In the first part we have to use the definition of the equivariant cohomology, which uses invariant currents. This definition is provided in the Appendix. If W_w were just an invariant smooth submanifold of Fl_n, we could regard the equivariant cohomology class $[W_w]$ as the equivariant Thom class of W_w. Unfortunately, W_w is not smooth. But we can talk about the current $\{W_w\}$, which is a sum of currents (one current for each face D with $w(D) = w$) and has some nontrivial singularities. It turns out that all the codimension one singularities of $\{W_w\}$ come in pairs with opposite orientations (two singularities for each ladder move.) So that $\partial_T\{W_w\} = 0$ and $[W_w]$ can be indeed defined.

More precisely, fix w and let $D_1, ..., D_r$ be all the reduced faces with $w(D_i) = w$. Let $C = (c_{i,j})$ be an $r \times r$ matrix with each $c_{i,j}$ being either 1 or 0, (1 if there is a ladder move, which changes D_i to D_j and 0 otherwise.) Clearly, the matrix C is symmetric.

If $c_{i,j} = 1$ then D_i and D_j differ by a single ladder move. Let's assume this ladder move is of size ℓ at the place (m, k). Let $D_{i,j}$ be the face whose triangular diagram contains all the equalities of D_i and D_j plus equalities $B_{m',k'}$, with $0 \leq m' - m - 1 = k' - k \leq \ell$ (examples are shown on Figure 4). Notice that $\dim D_i = \dim D_j = \dim D_{i,j} + 2$.

Lemma 2.4.2

$$\partial_T\{\Phi^{-1}(D_i)\} = \sum_{c_{i,j}=1} \{\Phi^{-1}(D_{i,j})\}. \tag{2.4}$$

Moreover, the orientations of $\Phi^{-1}(D_{i,j})$ induced by $\Phi^{-1}(D_i)$ and $\Phi^{-1}(D_j)$ are opposite.

Before proving the lemma, let us look at the two simplest examples, which will help to

explain the main ideas in the proof of this lemma.

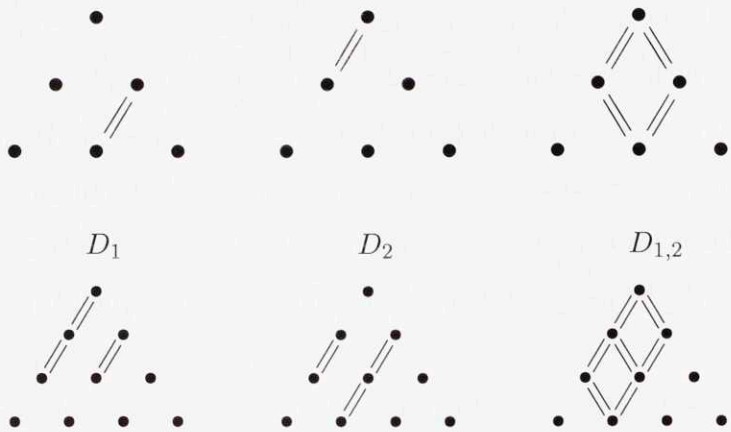

Figure 4: Ladder moves and faces which produce codimension one singularities.

Example 2.4.3 The first set of diagrams in Figure 4 corresponds to $n = 3$ and a ladder move of size 1. Label the diagrams by D_1, D_2 and $D_{1,2}$. It turns out that $\Phi^{-1}(D_{1,2})$ is just a three sphere S^3, and it is the boundary of both $\Phi^{-1}(D_1)$ and $\Phi^{-1}(D_2)$. Moreover, they induce different orientation on $\Phi^{-1}(D_{1,2})$. Hence, in this special case, Lemma 2.4.2 holds and implies that $\Phi^{-1}(D_1 \cup D_2)$ defines an honest cycle, which in turn defines an equivariant cohomology class.

Let us give a more detailed description of the codimension one singularity at $\Phi^{-1}(D_{1,2})$. We will show later that all codimension one singularities of general Φ look like the singularities on Fl_3 described below.

The Gelfand-Cetlin polytope $\Phi(Fl_3)$ in this case is shown on Figure 5. It has only one vertex with four edges coming out of it. This vertex is given by the diagram $D_{1,2}$ and it is the only non-smooth value of Φ.

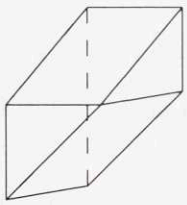

Figure 5: The Gelfand-Cetlin polytope for Fl_3.

Let us investigate the neighborhood of the singular sphere $S^3 = \Phi^{-1}(D_{1,2})$ in Fl_3 in details. It turns out that S^3 is Lagrangian and hence its small neighborhood is symplectomorphic to the neighborhood of the zero section of T^*S^3.

Introduce the following coordinates: $S^3 = \{(z_1, z_2) \in \mathbb{C}^2 |\ |z_1|^2 + |z_2|^2 = 1\}$. Let $z_1 =$

$x_1 + ix_2$ and $z_2 = x_3 + ix_4$. Then we can identify $T^*S^3 = \{(\xi, x) \in \mathbb{R}^4 \times \mathbb{R}^4 | \xi \perp x, |x| = 1\}$. Moreover, we have a Hamiltonian action of a two dimensional torus on T^*S^3 and another commuting Hamiltonian, which is not smooth on the zero section of T^*S^3. The two torus acts by $(\theta_1, \theta_2)(z_1, z_2) = (\theta_1 z_1, \theta_2 z_2)$, with $(\theta_1, \theta_2) \in S^1 \times S^1 \subset \mathbb{C} \times \mathbb{C}$. The two Hamiltonians for this action are $g_1 = x_1\xi_2 - x_2\xi_1$ and $g_2 = x_3\xi_4 - x_4\xi_3$. The third Hamiltonian is given by $f = \sqrt{\xi_1^2 + ... + \xi_4^2}$. Then, as expected, f is not smooth at $\xi = 0$. (Notice that f^2 is smooth, which coincides with the fact that $\lambda_{2,1} - \lambda_{3,1}$ is not smooth, while $(\lambda_{2,1} - \lambda_{3,1})^2$ is smooth on Fl_3.)

Moreover, we can choose the above coordinates so that $f = \lambda_{2,1} - \lambda_{3,1}$ while $g_1 + g_2 = 2\lambda_{2,0} - \lambda_{2,1} - \lambda_{3,1}$ and $g_1 - g_2 = 2\lambda_{3,2} - \lambda_{2,1} - \lambda_{3,1}$. Then $\Phi^{-1}(D_1)$ in the neighborhood of S^3 is just the submanifold of T^*S^3 where $f = g_1 + g_2$, which is given by: $\{(x, \xi) \in T^*S^3 | x_1 = \xi_2, x_2 = -\xi_1, x_3 = \xi_4, x_4 = -\xi_3, x_1 \geq 0\}$. Clearly, this manifold has boundary, which is the zero section of T^*S^3. Similarly, the boundary of $\Phi^{-1}(D_2)$ is also S^3, but the orientations induced on S^3 by $\Phi^{-1}(D_1)$ and $\Phi^{-1}(D_2)$ are going to be different. $\square$

Example 2.4.4 In the second row of Figure 4, $n = 4$ and the ladder move is of size 2. $\Phi^{-1}(D_{1,2})$ is of dimension 5, while both $\Phi^{-1}(D_1)$ and $\Phi^{-1}(D_2)$ are of dimension 6. Moreover $\Phi^{-1}(D_{1,2})$ is a part of boundaries of $\Phi^{-1}(D_1)$ and $\Phi^{-1}(D_2)$. But the orientations induced on $\Phi^{-1}(D_{1,2})$ by $\Phi^{-1}(D_1)$ and $\Phi^{-1}(D_2)$ are different. At the same time, $\Phi^{-1}(D_1 \cup D_2)$ does not define a closed cycle, since there are other codimension one singularities in $\Phi^{-1}(D_1)$, which come from ladder moves of size 1.

Let us carefully explain why $\partial_T\{\Phi^{-1}(D_2)\} = \{\Phi^{-1}(D_{1,2})\}$. The following argument will later be generalized in the proof of Lemma 2.5.

First of all let us rename the Gelfand-Cetlin coordinates for a 4×4 Hermitian matrix as shown in Figure 6 below, this will simplify the notations in this example.

$$\begin{array}{ccccccc} & & & \gamma & & & \\ & & \mu_1 & & \mu_2 & & \\ & \nu_1 & & \nu_2 & & \nu_3 & \\ \lambda_1 & & \lambda_2 & & \lambda_3 & & \lambda_4 \end{array}$$

Figure 6: The Gelfand-Cetlin coordinate on Fl_4.

Then the face D_2 is given by $\nu_1 = \mu_1$ and $\lambda_2 = \nu_2 = \mu_2$, while $D_{1,2}$ is given by $\nu_1 = \nu_2 = \mu_1 = \mu_2 = \lambda_2 = \gamma$. Let us introduce the faces F, G and H as shown on Figure

7. Face G is 4-dimensional (given by $\nu_1 = \mu_1$ and $\nu_2 = \mu_2$) and both D_2 and $D_{1,2}$ sit in G, so we will restrict our attention to $\Phi^{-1}(G)$. Clearly, F is contained in G as well. Let us also denote by G° the union of the interior of all subfaces F' of G such that F' intersects F nontrivially, then $G^\circ = G - H$.

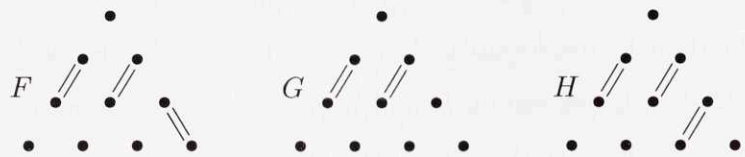

Figure 7: Faces F, G and H.

Actually, if we use the notation introduced in Section 2.2, we can see that F is equal to $F_{0,0,2}$. In particular, $\Phi^{-1}(F)$ is an embedded copy of Fl_3 in Fl_4 and contains all the Hermitian matrices with eigenvalues $\lambda_1, \lambda_2, \lambda_3, \lambda_4$ of the form shown below ($*$ indicates that any number can be places there given that other conditions are satisfied).

$$\begin{matrix} * & * & 0 & * \\ * & * & 0 & * \\ 0 & 0 & \lambda_4 & 0 \\ * & * & 0 & * \end{matrix}$$

Notice, that in the neighborhood of F, G is just a product of F and a one dimensional ray. This ray is just given by letting ν_3 vary and leaving the other coordinates fixed. The map, defined by the coordinate ν_3, is smooth in the neighborhood of $\Phi^{-1}(F)$ and is a moment map of a circle action S^1 in this neighborhood.

By local canonical form theorem (see, for example the book of Guillemin and Sternberg [15]) we know that we can choose a neighborhood $U_F \subset \Phi^{-1}(G)$ of $\Phi^{-1}(F) \subset \Phi^{-1}(G)$, which can be identified with a neighborhood of the zero section of some two dimensional symplectic vector bundle V over $Fl_3 = \Phi^{-1}(F)$. Then the action of the circle S^1 mentioned above is linear on the fibers and $\Phi^{-1}(F)$ is the fixed point set of this action. Moreover, the Gelfand-Cetlin action coordinates on U_F are given by ν_3 together with ν_1, ν_2, γ, which are the pullbacks from $\Phi^{-1}(F) = Fl_3$ of the Gelfand-Cetlin coordinates on Fl_3.

Set $D_2' = D_2 \cap F$ and $D_{1,2}' = D_{1,2} \cap F$. Then by Example 2.4.3, we know that $\partial\Phi^{-1}(D_2') = \Phi^{-1}(D_{1,2}')$. Moreover, since ν_1, ν_2, γ, are just the pullbacks from $\Phi^{-1}(F) = Fl_3$ we can conclude that $\Phi^{-1}(D_{1,2}) \cap U_F$ (or $\Phi^{-1}(D_2') \cap U_F$) is locally a product of $\Phi^{-1}(D_{1,2}')$

(respectively $\Phi^{-1}(D_2)$) and the fiber of V. Hence we proved

$$\partial(\Phi^{-1}(D_2) \cap U_F) = \Phi^{-1}(D_{1,2}) \cap U_F$$

In other words, $\Phi^{-1}(D_{1,2})$ is the boundary of $\Phi^{-1}(D_2)$ in the neighborhood of $\Phi^{-1}(F)$. Let us prove that the same holds if in the formula above we substitute U_F by $\Phi^{-1}(G^\circ)$ (set $\Phi^{-1}(G^\circ) = \tilde{U}$ and notice that ν_3 is smooth on $\tilde{U}$ and hence defines S^1 action on it). This will be enough to prove that $\partial_T\{\Phi^{-1}(D_2)\} = \{\Phi^{-1}(D_{1,2})\}$, since $\Phi^{-1}(G - G^\circ) \cap \Phi^{-1}(D_2)$ is of codimension at least 2 in $\Phi^{-1}(D_2)$ and hence cannot change the cohomology class.

To prove the above statement denote by $Z_a = \{A \in \tilde{U} | \nu_3(A) = a\}$. Then $M_a = Z_a/S^1$ is the reduction at a with respect to the S^1 action. (Recall, that the moment map of this action is ν_3). We can also define action coordinates on M_a. Indeed, restrict Φ to Z_a, then $\Phi|_{Z_a}$ is invariant with respect to S^1, hence we can define action coordinates Φ_a on M_a.

It is easy to see from the canonical local form theorem, that if a is close to λ_4, that is $Z_a \subset U_F$, then M_a is symplectomorphic to Fl_3 and action coordinates on M_a (denoted by Φ_a) are just the Gelfand-Cetlin action coordinates on Fl_3. Since ν_3 is smooth and has no critical points on the preimage of the interior of the face G, the same holds for every $\lambda_3 < a < \lambda_4$.

The neighborhood U_a of each Z_a can be identified with a neighborhood of the zero section of $Z_a \times \mathbb{R}$, where $\mathbb{R}$ is the dual of the the Lie algebra of S^1. And the Gelfand-Cetlin coordinates on this neighborhood are given by ν_3 and pullbacks of the coordinates on Z_a, while the coordinates on Z_a are just the pullbacks of the coordinates on M_a. So if $U_a \to M_a$ is the natural fibration, then the action coordinates on U_a are pullbacks of the action coordinates on M_a.

In particular, $\Phi^{-1}(D_2) \cap U_a$ is a smooth fibration over $\Phi_a^{-1}(D_2')$, where D_2' is the corresponding face in the three dimensional Gelfand-Cetlin polytope. The same holds for $D_{1,2}$, that is $\Phi^{-1}(D_{1,2}) \cap U_a$ is a smooth fibration over $\Phi_a^{-1}(D_{1,2}')$. But since by Example 2.4.3, we have $\partial(\Phi_a^{-1}(D_2)) = \Phi_a^{-1}(D_{1,2}')$, we conclude:

$$\partial(\Phi^{-1}(D_2) \cap U_a) = \Phi^{-1}(D_{1,2}) \cap U_a$$

This implies

$$\partial(\Phi^{-1}(D_2) \cap \tilde{U}) = \Phi^{-1}(D_{1,2}) \cap \tilde{U}$$

since $\tilde{U}$ can be covered by open sets U_a. This finishes the proof that $\partial_T\{\Phi^{-1}(D_2)\} = \{\Phi^{-1}(D_{1,2})\}$. $\square$

Proof. (of Lemma 2.4.2) We start with showing that if D_i is a reduced face then $\Phi^{-1}(D_i)\cap U$ is a smooth integrable manifold (recall that U is the open dense subset of Fl_n, where the Gelfand-Cetlin map is smooth). We know that Φ is an honest moment map on U, and since $\Phi^{-1}(D_i) \cap U$ is a connected component of the fixed point set of some subtorus of $T^{\frac{n(n-1)}{2}}$ action, we can show that $\Phi^{-1}(D_i)\cap U$ is symplectic (hence orientable) submanifold of dimension $2\dim(D_i)$. Moreover, it is clearly of finite volume and hence we can define integration over it, which defines $\{\Phi^{-1}(D_i)\}$.

Consider a ladder move at (m,k) of size ℓ, which changes D_i to D_j, so that the corresponding face $D_{i,j}$ produces a singularity of codimension 1. Let the face $G_{m,k,\ell}$ be given by a diagram containing equalities $A_{m',k'}$ with $m-k \leq m'-k \leq m-k+1$ and $k < k' < k+\ell$, so that this face contains faces D_i, D_j and $D_{i,j}$. (In Example 2.4.4 we have $G_{0,0,2} = G$.) Recall that $F_{m,k,\ell}$ was defined in section 2.2 and it is clear that $F_{m,k,\ell} \subset G_{m,k,\ell}$. Let us also define $G^{\circ}_{m,k,\ell}$ to be a subset of $G_{m,k,\ell}$ which contains the interior of all faces F' in $G_{m,k,\ell}$, which intersect nontrivially with $F_{m,k,\ell}$. (Again, in Example 2.4.4 $G^{\circ}_{0,0,2} = G^{\circ}$.)

Let $U_{i,j}$ be a subset of Fl_n, which is open and dense in $\Phi^{-1}(G_{m,k,\ell})$, such that most of the Gelfand-Cetlin coordinates on $U_{i,j}$ are smooth (that is $\lambda_{i,k} \neq \lambda_{i+1,k}$), but we allow $\lambda_{m+1,k+1} = \lambda_{m+2,k+1}$. Hence all the singularities on $U_{i,j}$ come from the non-smoothness of $\lambda_{m+1,k+1}$ and $\lambda_{m+1,k+2}$ when $\lambda_{m+1,k+1} = \lambda_{m+1,k+2}$. We will prove $\Phi^{-1}(D_{i,j})$ is an honest boundary of $\Phi^{-1}(D_i)$ on $U_{i,j}$ outside some set of codimension at least 2.

This will prove the Lemma, since all other singularities of $\Phi^{-1}(D_i)$ (those, which do not come from the ladder moves) are of codimension greater than one, real algebraic and hence do not change $\partial_T\{\Phi^{-1}(D_i)\}$. Actually, it is enough to prove this when D_i is of codimension $2\ell-1$ in the Gelfand-Cetlin polytope, (in other words it has the largest possible dimension given that the ladder move is of size ℓ.) Indeed, for other faces we just have to intersect D_i of codimension $2\ell-1$ with another face given by some equalities $A_{i,k}$, so that both $\Phi^{-1}(D_i)$ and $\Phi^{-1}(D_{i,j})$ are intersected transversely with the same manifold, which proves that $\Phi^{-1}(D_{i,j})$ is still a boundary of $\Phi^{-1}(D_i)$ in $U_{i,j}$. So, we will assume from now on that D_i has codimension $2\ell-1$.

Starting from this point we will proceed along the lines of the argument presented in

Example 2.4.4. Recall that the preimage of the face $F_{m,k,\ell}$ is Fl_3, which is embedded smoothly into Fl_n. Moreover, $U_{i,j}$ in the neighborhood of $\Phi^{-1}(F_{m,k,\ell})$ is just the preimage of the face $G_{m,k,\ell}$. Analogously to the circle action from Example 2.4.4, there is a smooth $\frac{n(n-1)}{2}-1-2\ell$ torus $\tilde{T}$ action on a neighborhood $U_{k,m,\ell} \subset U_{i,j}$ of the $\Phi^{-1}(F_{m,k,\ell})$, such that $\Phi^{-1}(F_{m,k,\ell})$ is the fixed point set of this action. (Notice $U_{m,k,\ell} \cap U_{i,j}$ was denoted by U_F in Example 2.4.4.) Moreover, the moment map $\tilde{\Phi}$ for this action is given by composing Φ with the projection of $\mathbb{R}^{\frac{n(n-1)}{2}}$ onto $\mathbb{R}^{\frac{n(n-1)}{2}}/\mathbb{R}^3$, where $\mathbb{R}^3$ are the three nontrivial directions of $F_{m,k,\ell}$. In particular, it is clear that we can extend the action of $\tilde{T}$ to $\Phi^{-1}(G^{\circ}_{m,k,\ell})$.

Hence, by local normal form theorem $U_{k,m,\ell}$ can be identified with a neighborhood of the zero section of a symplectic vector bundle V over Fl_3. Then, analogously to Example 2.4.4, we can conclude that locally, the singularities produced by $\Phi^{-1}(D_{i,j})$ in $\Phi^{-1}(D_i)$ are just the products of the corresponding singularities on Fl_3 and the fiber of the vector bundle V.

In other words, we can prove that in some small neighborhood of Fl_3 the preimage $\Phi^{-1}(D_{i,j})$ is going to be the boundary of both $\Phi^{-1}(D_i)$ and $\Phi^{-1}(D_j)$, that is

$$\partial(\Phi^{-1}(D_i) \cap U_{m,k,\ell}) = \Phi^{-1}(D_{i,j}) \cap U_{m,k,\ell}. \tag{2.5}$$

Moreover, the orientations on $\Phi^{-1}(D_{i,j})$ induced by $\Phi^{-1}(D_i)$ and $\Phi^{-1}(D_j)$ are opposite.

To finish the proof look at $\tilde{U}_{i,j} = \Phi^{-1}(G^{\circ}_{m,k,\ell})$ (here $\tilde{U}_{i,j}$ corresponds to $\tilde{U}$ in Example 2.4.4). Then $\tilde{U}_{i,j}$ is dense in $U_{i,j}$ and the difference $\Phi^{-1}(D_2) - (\Phi^{-1}(D_2) \cap \tilde{U}_{i,j})$ is at least of codimension 2 in $\Phi^{-1}(D_2)$. Hence it is enough to prove (2.5) with $U_{m,k,\ell}$ substituted by $\tilde{U}_{i,j}$.

Analogously to Example 2.4.4, denote by M_a the symplectic reduction of $\tilde{U}$ with respect to the $\tilde{T}$ action at a regular value $a \in \tilde{\Phi}(\tilde{U}_{i,j})$. Then, since $\tilde{\Phi}$ is smooth and has no critical points on the interior of the face $G_{m,k,\ell}$, M_a can be identified with Fl_3 and the neighborhood U_a of $Z_a = \tilde{\Phi}^{-1}(a)$ is a smooth fibration over M_a.

So, similarly to Example 2.4.4 we can prove (2.5) with $U_{m,k,\ell}$ substituted by U_a for regular values of a. It is also very easy to see by local canonical form theorem, that we can actually take any $a \in \tilde{\Phi}(\tilde{U}_{i,j})$. Since these U_a cover $\tilde{U}_{i,j}$, (2.5) holds with $\tilde{U}_{i,j}$ instead of $U_{m,k,\ell}$. This finishes the proof of the lemma. □

This lemma leads to the proof of the first part of the Theorem. Indeed, set $\{W_w\} = \sum_i \{\Phi^{-1}(D_i)\}$, then

$$\partial_T\{W_w\} = \sum_i \sum_{c_{i,j}=1} \{\Phi^{-1}(D_{i,j})\} = 0,$$

since C is symmetric, and each $\Phi^{-1}(D_{i,j})$ is counted twice and with the opposite orientations. So, $\partial_T\{W_w\} = 0$ and the equivariant cohomology class $[W_w]$ is well-defined.

For the second part of the theorem we need the following result of Kirwan (see [16]) about equivariant cohomology of Hamiltonian group actions, which is usually called the injectivity theorem.

Theorem 2.4.5 *Let M be a compact symplectic manifold with a Hamiltonian torus T action. Let $i : F \to M$ be the inclusion of the fixed point set of the T action. Then the map $i^* : H_T^*(M) \to H_T^*(F)$ is an injection.*

In other words to check that two equivariant cohomology classes on M are the same we just have to check that their restrictions to the fixed points are the same. Actually, in the case of flag manifold this result can be improved as follows.

Recall that we have identified the fixed point of the T action on Fl_n with the permutation group S_n. So that to each fixed point p (or nondegenerate vertex p) we associate a permutation w_p. Denote the restriction of a cohomology class h to the fixed point p by $h|_p$.

In the case of the flag manifold stronger version of the Kirwan injectivity theorem holds. The following proposition was proved by Goldin in [11]. (Our statement of it differs slightly from hers, since we had to adopt it to our notations and conventions.)

Proposition 2.4.6 *If $[W_w]|_p = [X_w]|_p$ for every p, for which w_p is not strictly greater than w (with respect to the Bruhat order), then $[W_w] = [X_w]$. Moreover, if $w_{p_0} = w$ then*

$$[X_w]|_{p_0} = \prod_{\alpha \in \Delta_+ \cap w\Delta_-} \alpha$$

where Δ_+ (or Δ_-) is the set of all positive (respectively negative) roots of $SU(n)$ and w acts on each α as an element of the Weyl group.

Since $[X_w]|_p = 0$ if $w_p \not\geq w$, all we have to prove to show that $[W_w] = [X_w]$ is the following two assertions:

1. W_w is supported outside of the fixed points p with $w_p \not\geq w$ and hence $[W_w]|_p = [X_w]|_p = 0$ for the fixed points $w_p \not\geq w$.

2. $[W_w]|_{p_0} = \prod_{\alpha \in \Delta_+ \cap w\Delta_-} \alpha$, where $w_{p_0} = w$.

The first statement is easy. Indeed, if some nondegenerate vertex p is contained in some reduced face D with $w(D) = w$, then the diagram of D sits inside the diagram of D_p (D_p was defined in Section 3) and we can write a reduced word for $w = w(D)$ which is a subword of $w_p = w(D_p)$, in other words $w_p \geq w$. Hence W_w is supported outside of all the points p with $w_p \not\geq w$.

To prove the second statement we have to understand how to compute $[W_w]|_{p_0}$ with $w_{p_0} = w$. Clearly, W_w is just an invariant smooth manifold in a neighborhood of p_0, since Φ is an honest moment map in the neighborhood of every fixed point and W_w is a preimage of the Gelfand-Cetlin face D_w in the neighborhood of p_0 (D_w is the only face with $w(D) = w$, which contains p_0). Let NW_w be the normal bundle of W_w in some small neighborhood of p_0. Then

$$[W_w]|_{p_0} = e_T(NW_w)|_{p_0} = e_T(NW_w|_{p_0})$$

where e_T denotes the equivariant Euler class. Since $NW_w|_{p_0}$ is just a vector space, the T action on it is given by some set of weights Λ. Moreover, it can be shown (see, for example, [14]) that

$$e_T(NW_w|_{p_0}) = \prod_{\alpha \in \Lambda} \alpha$$

So we just need to show that $\Lambda = \Delta_+ \cap w\Delta_-$.

Notice that Λ can be described as follows. $w\Delta_-$ is the set of weights of the T action on the tangent space $T_{p_0}Fl_n$. This set can be identified with the directions of the projections $P(e_{i,j})$ of all the edges $e_{i,k}$ of the Gelfand-Cetlin polytope, which come out of the nondegenerate vertex p_0. $\Lambda \subset w\Delta_-$, since $NW_w|_{p_0}$ is a subspace of $T_{p_0}Fl_n$. Moreover, Λ contains only those weights which come from edges which are not contained in the Gelfand-Cetlin face D_w. But these edges are exactly those which are constructed from the diagram of p by removing the equalities $A_{i,k}$. Thus we can apply Proposition 2.2.2 to show that $\Lambda = \Delta_+ \cap w\Delta_-$.

This finishes the proof of Theorem 2.4.1.

2.5 Formulas for double Schubert polynomials.

In this section we give formulas for computing Schubert and double Schubert polynomials in terms of reduced faces of the Gelfand-Cetlin polytope. The classical Schubert polynomials were introduced by Bernstein, Gelfand, Gelfand in [3] and by Lascoux, Schutzenberger in [19]. An exposition of the theory of double Schubert polynomials can be found in a book by Macdonald [20].

First of all we will recall some well known facts about the T equivariant cohomology ring of Fl_n. It is given by

$$H_T^*(Fl_n) = \frac{\mathbb{C}[x_1, ..., x_n, y_1, ..., y_n]}{\prod(1+x_i) - \prod(1+y_i), \sum x_i}$$

where, morally speaking, the x_i's are the variables which come from the torus action (the equivariant cohomology of a point is equal to $\frac{\mathbb{C}[x_1,...,x_n]}{\sum x_i}$, the x_i's can also be thought of as the coordinates on the dual of the Lie algebra $\mathfrak{t}^*$) and the y_i's are the variables which come from the regular cohomology of Fl_n. We will denote the quotient map from $\mathbb{C}[x,y] \to H_T^*(Fl_n)$ by f. It can be shown that $f(x_i)|p = x_i$ and $f(y_i)|p = x_{w_p^{-1}(i)}$ for every $p \in Fl_n^T$. More details can be found in [11].

There is an iterative procedure which allows us to define double Schubert polynomials $P_w(x,y) \in \mathbb{C}[x,y]$ such that these polynomials represent cohomology classes $[X_w] \in H_T^*(Fl_n)$, that is $f(P_w(x,y)) = [X_w]$.

We define a divided difference operator ∂_i, which acts on a polynomial $P(x,y)$ by:

$$\partial_i P = \frac{P - s_i P}{x_{i+1} - x_i},$$

where s_i acts on P by interchanging x_i with x_{i+1}. Then if $w = s_{i_1}...s_{i_k}$ is a reduced expression for w we define $\partial_w = \partial_{i_1}...\partial_{i_k}$. It is easy to see that ∂_w does not depend on a reduced expression of w. Then we define $P_{w_0} = \prod_{i+j \leq n}(y_j - x_i)$, where w_0 is the longest permutation, and

$$P_w = \partial_{w^{-1}w_0} P_{w_0}.$$

These are called double Schubert polynomials and they satisfy $f(P_w(x,y)) = [X_w]$.

For every reduced face D let us define a polynomial $P_D(x,y)$ as follows. We label each equality $A_{i,k}$ by the monomial $y_{i-k} - x_{k+1}$ (see Figure 8 for $n = 4$). Then P_D is equal to

the product of all the monomials which are contained in D. For example, for the second diagram from picture 1 this polynomials is $(y_1 - x_1)(y_1 - x_2)$.

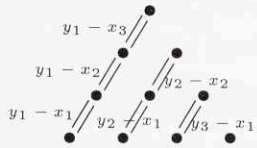

Figure 8: Labeling the diagram by monomials

Now, we are ready to state the following theorem.

Theorem 2.5.1 *For a permutation w, P_w is equal to the sum of P_D with $w(D) = w$, that is*

$$P_w = \sum_{w(D)=w} P_D.$$

We will omit the proof of this theorem, since it was proved by Fomin and Kirillov in [7] and several modifications of this result also appeared in [8], [4], [1]. We have yet another combinatorial argument which proves this theorem, but this argument does not seem to explain the theorem any better than already known proofs. At the same time it is clear that there should be a purely geometric proof of this theorem, which is based on the new cycles for Schubert polynomials constructed in Theorem 2.4.1 and the Kirwan injectivity theorem. We were not able to find this geometric argument. But the proof of Theorem 2.6.1 in the next section suggests that such an argument should exist.

Remark 2.5.2 If we set the y_i's equal to zero we get regular Schubert polynomials, actually $S_w = (-1)^{l(w)} P_w(x, 0)$ will be the classical Schubert polynomials. The above theorem clearly provides a rule for computing Schubert polynomials and not only double Schubert polynomials.

2.6 Other cohomology classes constructed using faces of the Gelfand-Cetlin polytope.

Until this point we have been looking only at the very special faces of the Gelfand-Cetlin polytope. It is interesting to see if other faces can be incorporated into a more general picture. In this section we provide one example of the construction of equivariant cohomology

classes on Fl_n, which are different from the Schubert classes, using faces of the Gelfand-Cetlin polytope. We will do this for the equivariant cohomology class given by $y_i - x_k$ with $i + k \leq n$. This example suggests that it might be possible to construct a much wider set of equivariant cohomology classes using the Gelfand-Cetlin polytope.

In this section we will work with only those faces which are given by a single equality $A_{i,k}$ or $B_{i,k}$, we will denote these faces by $D^A_{i,k}$ and $D^B_{i,k}$ respectively.

For i, k with $i + k \leq n$, define two unions of faces

$$F_{i,k} = D^A_{i+k-1,k-1} \bigcup (\cup_{i',k'} D^B_{i',k'})$$

with $k' \leq k - 2$ and $i' - k' = i + 1$ and

$$G_{i,k} = \bigcup_{i',k'} D^B_{i',k'}$$

with $k' \leq k - 1$ and $i' - k' = i$. Then

Theorem 2.6.1 *The current*

$$T_{i,k} = \{\Phi^{-1}(F_{i,k})\} - \{\Phi^{-1}(G_{i,k})\}$$

is closed and defines an equivariant cohomology class on Fl_n. Moreover,

$$[T_{i,k}] = f(y_i - x_k).$$

Proof. Using the same argument as in the proof of Theorem 2.4.1 we can prove that $\partial_T(T_{i,k}) = 0$. Again, the preimage of each face has codimension one singularities, but they all cancel out at the end, since each singularity is counted twice and with the opposite signs.

To show that $[T_{i,k}] = f(y_i - x_k)$ we will prove that for each fixed point p of the T action on Fl_n,

$$[T_{i,k}]|_p = f(y_i - x_k)|_p.$$

This will be enough to prove the theorem by the Kirwan injectivity Theorem 2.4.5.

We know that

$$f(y_k - x_i)|_p = x_{w_p^{-1}(i)} - x_k.$$

We will prove by induction on n that

$$[T_{i,k}]|_p = x_{w_p^{-1}(i)} - x_k. \tag{2.6}$$

When $n = 2$ this is easy. Let's assume we have proved it for $n-1$ and we need to prove it for n.

If $B_{i',k'}$ (or $A_{i',k'}$) is a part of the diagram for the nondegenerate vertex p, then the equivariant cohomology class in a small neighborhood of the fixed point p of the restriction $\{\Phi^{-1}(D^B_{i',k'})\}|_p$ (respectively $\{\Phi^{-1}(D^A_{i',k'})\}|_p$) is given by the root, which is pointing in the direction of the projection $P(e_{i',k'})$ of the corresponding edge $e_{i',k'}$ coming out p. If $B_{i',k'}$ (or $A_{i',k'}$) is not a part of p then this restriction is 0.

This fact can be used as follows. Let the nondegenerate vertex p have j_1 equalities $A_{i,0}$ in the bottom row of its diagram. Then $w_p = uw_{\tilde{p}}$, where $u = s_{j_1}...s_1$ and $w_{\tilde{p}}$ is the permutation on the elements $2, ..., n$, which is constructed by removing the bottom row of the diagram of p and taking the permutation of the new diagram $\tilde{p}$. Then, by the induction assumption, we can conclude:

$$[T_{i,k}]|_p = x_{w_{\tilde{p}}^{-1}(i+1)} - x_k + \alpha_1 + \alpha_2 \tag{2.7}$$

where α_1, α_2 are the weights which come from the restrictions of $D^B_{i,0}$ and $D^B_{i+1,0}$ to p respectively (these weights might be equal to 0).

We will look at three cases:

1. $j_1 \geq i$.

2. $j = i$.

3. $j < i$.

In the first case, p is not contained in $D^B_{i,0}$ and $D^B_{i+1,0}$ so both α_1 and α_2 are zero. Moreover, $w^{-1}(i) = w_{\tilde{p}}^{-1}(i+1)$ (remember, that $w_{\tilde{p}}$ permutes $2, ..., n$), so inserting this information in (2.7) we get (2.6).

In the second case, $p \in D^B_{i+1,0}$, but not in $D^B_{i-k,0}$. So $\alpha_1 = 0$ and $\alpha_2 = x_1 - x_{w_p^{-1}(i+1)}$. Plugging this into (2.7) and using $w_{\tilde{p}}^{-1}(i+1) = w_p^{-1}(i+1)$ we get

$$[T_{i,k}]|_p = x_{w_{\tilde{p}}^{-1}(i+1)} - x_k + x_1 - x_{w_p^{-1}(i+1)} = x_1 - x_k$$

which proves (2.6), since in this case $w_p^{-1}(i) = 1$

For the third case, p is contained in both $D^B_{i,0}$ and $D^B_{i+1,0}$ so $\alpha_1 = -(x_1 - x_{w_p^{-1}(i)})$ and $\alpha_2 = x_1 - x_{w_p^{-1}(i+1)}$. Moreover $w_{\tilde{p}}^{-1}(i+1) = w_p^{-1}(i+1)$. So we have:

$$[T_{i,k}]|_p = x_{w_{\tilde{p}}^{-1}(i+1)} - x_k - (x_1 - x_{w_p^{-1}(i)}) + x_1 - x_{w_p^{-1}(i+1)} = x_{w_p^{-1}(i)} - x_k$$

which is exactly (2.6).

There is only one situation left to check, that is when $k = 1$. Then $F_{i,1}$ is just one face $D^A_{i,0}$, while $G_{i,1}$ is also one face $D^B_{i,0}$. Every nondegenerate vertex p is contained in exactly one of the two faces. If $p \in D^A_{i,0}$, then $P(e_{i,0})$ produces the weight $x_{w_p^{-1}(i)} - x_1$, while if $p \in D^B_{i,0}$, then $P(e_{i,0})$ points in the direction of $x_1 - x_{w_p^{-1}(i)}$, but we have to take $\Phi^{-1}(G_{i,1})$ with the minus sign. So (2.6) holds for any i when $k = 1$.

This finishes the induction and the proof of the Theorem. $\square$

Chapter 3

RC-graphs and Littlewood-Richardson Rule

3.1 RC-graphs and Young Tableaux.

In this section we give a combinatorial description of RC-graphs, show that they can be identified with reduced faces of the Gelfand-Cetlin polytope and explain how Young tableaux can be thought of as RC-graphs of permutations constructed out of partitions.

We start with a definition of RC-graphs. (Our conventions are not standard and differ from the conventions in [1] and [7], since we've chosen them to fit the standard notations for Young tableaux.) Let R be a finite set of pairs of integers $R = \{(i,k) | i \leq n, k \leq n\}$ (both i, k can be negative). We will think of R as a table of intersecting and nonintersecting strands. Strands intersect for each $(i,k) \in R$ and do not intersect otherwise. The examples are provided on Figure 9, where we have three tables of strands $R_1 = \{(2,1),(1,1),(-1,2)\}$, $R_2 = \{(3,1),(2,3),(1,2)\}$ and $R_3 = \{(3,2),(2,2),(1,2),(2,3)\}$.

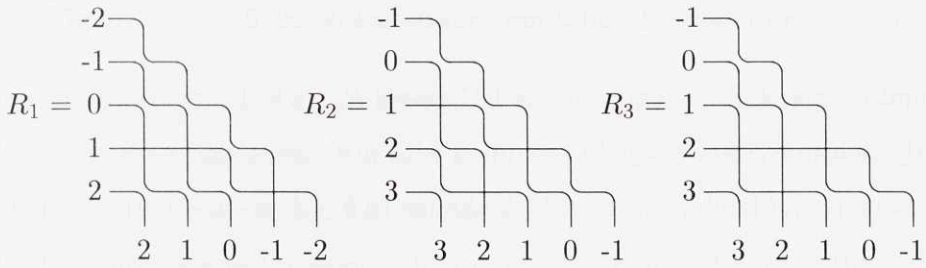

Figure 9: Examples of RC-graphs.

R is called an RC-graph if no two strands intersect twice. We can think of each RC-

graph as a planar history of a permutation w_R, which is defined as follows. If we label each strand by the row where it starts from, then $w_R(i)$ is given by the column, where i^{th} strand ends. Each w_R permutes all the integers, which are less than or equal to n. There always exists some negative N such that $w_R(i) = i$ for $i < N$.

It is also very simple to see that R also provides a reduced expression for w_R, in other words we can write w_R in terms of a minimal length product of simple transpositions. One way to do it is to read each row of the RC-graph from right to left, from the bottom row to the top one and multiply out simple transpositions $s_{i+k-n-1}$ for each $(i,k) \in R$ (each s_j interchanges j and $j+1$ and j might be negative).

For example, for the RC-graphs from Figure 9, the corresponding permutations are given by $w_{R_1}(2,1,0,-1,-2) = (2,-2,1,0,-1)$ with $w_{R_1}(i) = i$ for $i < -2$, $w_{R_2}(3,2,1,0,-1) = (3,1,-1,2,0)$ with $w_{R_2}(i) = i$ for every $i < -1$ and finally $w_{R_3}(3,2,1,0,-1) = (3,-1,1,2,0)$ with $w_{R_3}(i) = i$ for every $i < -1$.

Each reduced face D of the Gelfand-Cetlin polytope can be identified with an RC-graph. Indeed, we can change each equality $A_{i,k}$ in the diagram of D by an intersecting strand at the place $(n+k-i, n-k)$ and all other inequalities by nonintersecting strands and then connect the strands. It is easy to see that this constructs an RC-graph for each reduced face.

So, let us repeat some properties of RC-graphs, which have already been stated in the language of reduced faces in Section 3:

- Let R be an RC-graph, such that $(i,k), (i-1,k)$ and $(i-1,k-\ell)$ are not in R for some i,k and ℓ, but all other (i',k') with $k \geq k' \geq k+\ell$ and $i \geq i' \geq i+1$ are in R. Then we can substitute $(i,k-\ell)$ by $(i-1,k)$ without changing w_R. (We also can go backwards.) These operations are called *ladder moves* of size ℓ at the place (i,k). Examples of ladder moves of sizes 1 and 2 are shown on Figure 10

- For every permutation w there exist a unique RC-graph R_w (which we will call a *top RC-graph* of w), such that every other RC-graph R with $w_R = w$ could be constructed from R_w by a sequence of ladder moves, which change $(i,k-\ell)$ to $(i-1,k)$ (but not the other way).

- Each top RC-graph R_w has the property that if $(i,k) \in R_w$ and $i \leq n$, then $(i+1,k) \in R_w$. In other words, all intersecting strands of R_w are concentrated strictly to the left

in each row of R_w.

Figure 10: Examples of ladder moves on RC-graphs of sizes 1 and 2.

From now on we will only work with those permutations w for which $w(i) > w(i-1)$ for each $i \leq 0$. Equivalently, every RC-graph R with $w_R = w$ can be defined by the following property:

- R has no two nonpositive intersecting strands.

In particular, if R satisfies the above property it lies below the 0th row, that is if $(i,k) \in R$ then $k \geq 1$. This shows that the above property just says that we do not want to consider any permutations w which have RC-graphs partially located above the zeroth row. Let us emphasize that starting from this point every RC-graph mentioned in this text has to satisfy the above property. In particular, the property is implicitly assumed in all the statements of theorems and lemmas stated below.

Let us now define Young diagrams and tableaux. A Young diagram will be given by a partition $\mu = (\mu_1, ..., \mu_n)$, where $\mu_1 \geq \mu_2 \geq ... \geq \mu_n$. Graphically it will be given by μ_i boxes in i^{th} row, as shown on the Figure 11, where Young diagrams correspond to partitions $\mu_1 = (3)$, $\mu = (2,1)$ and $\mu_3 = (3,1,1)$ respectively.

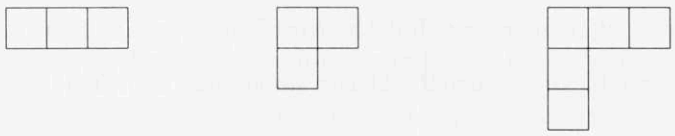

Figure 11: Examples of Young diagrams.

A Young tableaux Y is a filling of a Young diagram with numbers $1, ..., n$ which satisfies the following properties. If a and b are two boxes of the Young diagram, which lie in the same row, and a is to the left of b then the number in a is not greater than the number in b. If a and b are in the same column and a is on top of b, then the number in a should be strictly less than the number in b. We denote by $\mu(Y)$ the partition, which corresponds to the Young tableaux Y. Examples of Young tableaux are shown on Figure 12.

$$Y_1 = \begin{array}{|c|c|c|}\hline 1 & 1 & 2 \\ \hline \end{array} \qquad Y_2 = \begin{array}{|c|c|}\hline 1 & 3 \\ \hline 3 \\ \cline{1-1} \end{array} \qquad Y_3 = \begin{array}{|c|c|c|}\hline 1 & 2 & 2 \\ \hline 2 \\ \cline{1-1} 4 \\ \cline{1-1} \end{array}$$

Figure 12: Examples of Young tableux.

Given a partition μ, we construct an RC-graph $R(\mu)$ as follows. Let $R(\mu) = \{(i,k)|1 \leq k \leq n, n \geq i \geq n - \mu_k + 1\}$. Then, set $w(\mu) = w_{R(\mu)}$. $R(\mu)$ is going to be the top RC-graph of $w(\mu)$. Every such permutation has a unique ascent at 0, that is $w(1) < w(0)$ but $w(i) > w(i-1)$ if $i \neq 1$ In particular every permutation $w(\mu)$ satisfies $w(i) > w(i-1)$ if $i \leq 0$. The following lemma shows why we can think about RC-graphs as about generalizations of Young diagrams (similar results were obtained by Winkel in [24]).

Lemma 3.1.1 *RC-graphs R with $w_R = w(\mu)$ are in one to one correspondence with Young tableaux Y with $\mu(Y) = \mu$.*

Proof. It is easy to see that we can apply only ladder moves of size 1 to any R with $w_R = w(\mu)$. Start with the top RC-graph $R(\mu)$ and the top Young diagram, which is given by filling the ith row of the Young diagram with entries i. Associate to each ladder move of size 1 an increase by 1 of the corresponding box in the Young tableaux. This obviously constructs a one to one correspondence between RC-graphs with permutation $w(\mu)$ and Young tableaux with partition μ. □

Denote by $R(Y)$ the RC-graph, which is constructed out of the Young tableau Y. As an illustration to the above lemma let us mention that the first Young tableau Y_1 on Figure 12 correspond to the first RC-graph R_1 on Figure 9. At the same time $w(\mu(Y_2)) = w_{R_2}$ but $R(Y_2) \neq R_2$.

Call any finite sequence of numbers $1, ..., n$ a *word*. For each Young tableau Y, associate a word $v(Y)$, which is given by reading the entries of the tableau from left to right in each row, starting from the bottom row and going to the top one. For example, the words of Young diagrams from Figure 12 are $v(Y_1) = 112$, $v(Y_2) = 313$ and $v(Y_3) = 42122$.

On the set of all words we define Knuth moves (originally they appeared in [17]). These Knuth moves allow the following changes to a word:

$$...yxz... \Leftrightarrow ...yzx... \quad \text{if} \quad x < y \leq z$$

and

$$...xzy... \Leftrightarrow ...zxy... \text{ if } x \leq y < z$$

We say that two words v_1 and v_2 are Knuth equivalent if we can go from one of them to another by applying a sequence of Knuth moves.

The following theorem is the key fact in the Littlewood-Richardson rule for multiplying Schur polynomials and will be extremely useful to us. The proof of it can be found in [9].

Theorem 3.1.2 *If Y_1 and Y_2 are two distinct Young tableaux then $v(Y_1)$ and $v(Y_2)$ are not Knuth equivalent. Moreover, each word v is Knuth equivalent to exactly one word $v(Y)$.*

At the end of this Section we recall the definitions of Schur and Schubert polynomials. Each Young tableaux Y defines a monomial x^Y, which is equal to the product of x_i's with one x_i for each entry i in the tableaux. Each partition μ defines a Schur polynomial

$$S_\mu = \sum_{\mu(Y)=\mu} x^Y.$$

It is well known that Schur polynomials are symmetric polynomials and that they form a basis for the space of symmetric polynomials in n variables.

Similarly, given an RC-graph R we define x^R to be the product of x_k's with one x_k for each $(i,k) \in R$. Then the Schubert polynomial for the permutation w is given by

$$S_w = \sum_{w_R=w} x^R.$$

Polynomials S_w form a basis for the space of all polynomials in n variables.

Since $x^{R(Y)} = x^Y$, Proposition 3.1.1 implies that $S_{w(\mu)} = S_\mu$, in other words we can think of Schubert polynomials as generalizations of Schur polynomials.

3.2 Insertion Algorithm

The key tool in the classical Littlewood-Richardson rule for multiplying Schur polynomials is the Schensted insertion algorithm. This algorithm was generalized to the case of RC-graphs in [1] and used to prove Monk's formula. We will show that in a special case, this generalized algorithm can be used to provide the Littlewood-Richardson rule for multiplying

some Schubert polynomials by Schur polynomials. This section defines the algorithms and discusses its basic properties.

Let R be an RC-graph. We would like to provide an algorithm for inserting a number $1 \leq k \leq n$ into R.

Let us call a pair (i, j) an *open space*, if $(i, j) \notin R$ (two strands at position (i, j) do not intersect) and the top strand of the intersection is labeled by a nonpositive number, while the bottom strand is labeled by a positive number. (See Figure 13.)

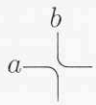

Figure 13: An example of an open space: $a > 0 \geq b$.

Start at the row number $k_1 = k$ and find the smallest i_1 such that the space (i_1, k_1) is open (sometimes we will write $(i_1(k), k_1(k))$ to indicate the dependence on k). Insert (i_1, k_1) into R, in other words change the corresponding nonintersecting strands to intersecting. If a, b are the two labels of the strands going through the place (i_1, k_1) we set $a_1(k) = a$ and $b_1(k) = b$. If we constructed an RC-graph we stop, otherwise, it is easy to see that the two stands which now intersect at the place (i_1, k_1) must also intersect at some other place (ℓ_2, k_2) with $k_2 > k_1$. Then we remove (ℓ_2, k_2) from R and find the smallest $i_2 > \ell_2$ such that (i_2, k_2) is open (we can find such i_2, since the strand labeled by $b_1 \leq 0$ passes through the row k_2 to the left of (ℓ_2, k_2) and the row k_2 also has a positive strand to the left of the strand labeled by b_1). We insert (i_2, k_2) into R (again, sometime we denote it by $(i_2(k), k_2(k))$), set $a_2(k)$ and $b_2(k)$ to be the labels of the strands passing through (i_2, k_2) and continue the process until it stops. For notational convenience set $k_{j+1}(k) = n + 1$, if the last intersection we inserted was $(i_j(k), k_j(k))$.

The resulting RC-graph will be denoted by $R \leftarrow k$. Note, $R \leftarrow k$ and R have the same number of crossings in each row, except for the row k, where $R \leftarrow k$ has an additional crossing. This immediately leads to the following consequence

$$x^R x_k = x^{R \leftarrow k}.$$

If v is a word, we denote by $R \leftarrow v$ the RC-graph we get after inserting one by one the letters of v. If Y is a Young tableau, we say $R \leftarrow Y = R \leftarrow v(Y)$. Obviously we have:

$$x^R x^Y = x^{R \leftarrow Y}.$$

The above algorithm is a generalization of the Schensted insertion algorithm, which originally appeared in [23]. To prove this we just have to translate what this algorithm means in the language of Young tableaux, in the case when $R = R(Y)$ is constructed from some young tableau Y as in Lemma 3.1.1. We omit the simple technical details of this proof, but recall a very important fact about this algorithm (see [9]). For two Young tableaux Y_1 and Y_2 we have

$$v(Y_1 \leftarrow Y_2) \text{ is Knuth equivalent to } v(Y_1)v(Y_2). \tag{3.1}$$

where $v(Y_1)v(Y_2)$ is just the concatenation of the two words $v(Y_1)$ and $v(Y_2)$.

Let us introduce a few new notations, which will be used later. During the insertion algorithm of k into R, each place (i_j, k_j) was connected to (ℓ_{j+1}, k_{j+1}) by two pieces of strands s_j and s^j. (Let us emphasize that s_j and s^j are just pieces of strands, which are between rows k_j and k_{j+1} and their labels change during the insertion.) We say that the left strand s_j is a part of the left path $\ell(k)$ of the insertion while the right strand s^j is a part of the right path $r(k)$ of the insertion. Both $\ell(k)$ and $r(k)$ are collections of pieces of stands. The labeling of each piece s_j in $\ell(k)$ changes from being positive a_j to nonpositive b_j, while the labeling of s^j in $r(x)$ change from b_j to a_j.

Lemma 3.2.1 *If no two nonpositive strands intersect in R, then no two nonpositive strands intersect in $R \leftarrow k$.*

Proof. During the insertion algorithm the only possibility for introducing new intersections of nonpositive strands is when a strand s_j from $\ell(k)$ becomes nonpositive.

Let us show by contradiction that s_j cannot intersect any nonpositive strand. Assume that s_j (labeled by $b_j \leq 0$) in $R \leftarrow k$ is intersected by some nonpositive strand s in row $k_j < k' < k_{j+1}$. Look at the whole strand s' in $R \leftarrow k$, which is labeled by a. s' starts below zero, while s starts above zero, at the same time s is to the left of s' in the row k', hence these two strands must intersect in $R \leftarrow k$ above the row k'. The strand s' above the

row k' consists of two parts: one of them is s^j, which was labeled by b in R, and the other one is the rest of the strand above the row k_j, which is labeled by a in both R and $R \leftarrow k$.

s cannot intersect s^j, since no two nonpositive strands intersect in R. At the same time s cannot intersect the rest of s', since it already intersects the strand labeled by a in R once, and cannot intersect it for the second time. So we found a contradiction and this lemma is proved. □

The lemma immediately leads to the following property

- All strands passing between $r(k)$ and $\ell(k)$ are positive.

Indeed, each strand between $r(k)$ and $\ell(k)$ has to cross at least one strand from $r(k)$ or $\ell(k)$, but, since $r(k)$ is nonpositive in R and $\ell(k)$ is nonpositive in $R \leftarrow k$, and no two nonpositive strand can intersect, the above property holds.

Here is a very important lemma, which does not hold in the case of the more general algorithm given in [1].

Lemma 3.2.2 *If $x \leq y$, then the path of x is weakly to the left of the path of y in $R \leftarrow xy$.*

If $x > y$ then the path of x is weakly to the right of the path of y in $R \leftarrow xy$.

Remark 3.2.3 When we say that the path of x is to the left (right) of the path of y, we imply that the right path of x is to the left of the left path of y (respectively, the left path of x is to right of the right path of y). The word *weakly* stands for the fact that $r(x)$ and $\ell(y)$ (respectively $\ell(x)$ and $r(y)$) might have some common parts of some strands.

Proof. For the case $x \leq y$ the right path $r(x)$ of x in $R \leftarrow x$ contains strands which are all greater than zero after the insertion. Thus when we start inserting y into $R \leftarrow x$ each row $k \geq x$ should contain an open space to the right of the right path of x (since the right path of x is positive). Hence the left path of y is going to stay strictly to the right of the right path of x, until at some point it might happen that left path of y is the same as the right path of x.

It can occur only when an open space $(i, k) = (i_j(y), k_j(y))$ in $R \leftarrow x$ contains strands $s_j(y)$ and $s^j(y)$, such that part of $s_j(y)$ is a part of $r(x)$. In other words, $s_j(y)$ and $s^{j'}(x)$ have some common parts. If the insertion algorithm stops at this point there is nothing else to prove. Otherwise, there should be a place $(i_{j+1}(y), k_{j+1}(y))$ where strands $s_j(y)$ and

$s^j(y)$ intersect again. We would like to show that

$$k_{j+1}(y) > k_{j'+1}(x). \tag{3.2}$$

This will imply that the path of y at the row k_{j+1} is strictly to the right of the path of x and (3.2) will be enough to prove the first part of the lemma. Indeed if $r(x)$ and $\ell(y)$ coincide at some row k, they have to separate at the row $k_{j'+1}(x)$ by (3.2) and $r(x)$ have to stay to the left of $\ell(y)$. If they coincide again at some lower row, we can repeat the argument and show that they have to separate again.

$s^{j'}(x)$ was nonpositive in R, hence it cannot intersect s^j, which was also nonpositive in R. Thus if $s_j(y)$ and $s^j(y)$ intersect again, it should happen below the row where $s^{j'}(x)$ ends, in other words, below the row of intersection of $s_{j'}(x)$ and $s^{j'}(x)$, but this row is exactly $k_{j'+1}(x)$. Therefore (3.2) holds and the first part of the lemma is proved.

In the case $x > y$, the right path of y gets changed from being a set of nonpositive strands to positive strands. The left path of x in $R \leftarrow x$ contains only nonpositive strands after the insertion, so these two paths cannot intersect (but some parts of them can coincide), since no two nonpositive strands can intersect.

Let's now argue by contradiction that $r(y)$ is weakly to the left of $\ell(x)$ using the fact that $r(y)$ cannot intersect $\ell(x)$. Pick the smallest k, such that the right path of y is to the right of the left path of x. This could not happen because of an intersection of $r(y)$ and $\ell(x)$. Thus in the row k the insertion of x into R had to remove some $(\ell_j(x), k_j(x)) = (\ell_j(x), k)$ from R and add some $(i_j(k), k)$ to R, moving $\ell(x)$ to the left. But only nonpositive strands pass in row k between $\ell_j(x)$ and $i_j(k)$ (otherwise, we would get an open space there, which is impossible), hence $r(y)$ cannot pass between $\ell_j(x)$ and $i_j(x)$ and it must coincide with $\ell(x)$ in the row $k-1$). Moreover, the strand passing the row k directly to the left of $(\ell_j(x), k)$ is nonpositive in $R \leftarrow x$. At the same time, the strands between right and left paths of y are always positive, so the strand passing the row k directly to the left of $(\ell_j(x), k)$ is positive. We found a contradiction, which means that the second part of the lemma is proved. □

This Lemma immediately proves that if $0 < x < y \leq z \leq n$ then

$$R \leftarrow yxz = R \leftarrow yzx \tag{3.3}$$

Indeed in $R \leftarrow yx$ we know that $\ell(y)$ is weakly to the right of $r(x)$, so $r(y)$ is unchanged when we insert x into $R \leftarrow y$. At the same time when we insert z in $R \leftarrow y$ the left path $\ell(z)$ is weakly to the right of $r(y)$. So, paths of x and z are separated by the path of y and, in particular, do not have any common strands. Hence multiplication of $R \leftarrow y$ by x commutes with multiplication by z, which proves (3.3).

Thus if v_1 and v_2 are two Knuth equivalent words, which can be gotten from one another using only Knuth moves of the first type, we have

$$R \leftarrow v_1 = R \leftarrow v_2$$

Let us talk about how the permutation of R changes after insertion. Notice that after each step of the algorithm the permutation w_R does not change except for the last step. At the end we make two nonintersecting stands labeled by c and d intersect, which means that

$$w_{R \leftarrow x} = s_{c,d} w_R$$

where $s_{c,d}$ is the transposition (with $c > 0 \geq d$), which interchanges c and d, when it acts on a permutation from the right. Moreover,

$$l(s_{c,d} w_R) = l(w_R) + 1$$

Conversely, given an RC-graph R' with $w_{R'} = s_{c,d} w_R$, such that $l(s_{c,d} w_R) = l(w_R) + 1$ and $c > 0 \geq d$ we can traverse the above algorithm backwards starting by finding the unique intersection of strands labeled by c and d, making them nonintersecting and then proceeding in the opposite order. For more details about the inverse of the insertion algorithm see [1].

This immediately leads to a special case of the Monk's formula (the more general case of Monk's formula was proved using the more general algorithm in [1]). We postpone the proof of the following theorem until the proof of the more general statement in Lemma 3.3.2.

Theorem 3.2.4

$$S_w \cdot (x_1 + ... + x_n) = \sum_{c > 0 \geq d} S_{s_{c,d} w}$$

where the sum is taken over all pairs (c, d) *with* $l(s_{c,d} w) = l(w) + 1$.

3.3 Littlewood-Richardson rule for multiplication Schubert polynomials by Schur polynomials.

Given a Schur polynomial S_μ and a Schubert polynomials S_w their product can be uniquely written as a sum of Schubert polynomials:

$$S_w S_\mu = \sum_u c^u_{w,\mu} S_u,$$

where the sum is taken over all the permutations u. The coefficients $c^u_{w,\mu}$ are called Littlewood-Richardson coefficients and are known to be positive. The following theorem provides a rule for computing these coefficients:

Theorem 3.3.1 *Let w be a permutation, which satisfies $w(i) > w(i-1)$ for each $i \leq 0$ and let μ be any partition. Choose any RC-graph U and set $w_U = u$. Then $c^u_{w,\mu}$ is equal to the number of pairs (R, Y) of an RC-graph R and a Young tableau Y with $w(R) = w$ and $\mu(Y) = \mu$, such that $R \leftarrow Y = U$.*

The next three lemmas will lead to the proof of the above theorem. Let us define a Young diagram ν_m to be just one row of m boxes, so that the corresponding partition is given by one number m.

Lemma 3.3.2 *Theorem 3.3.1 holds when $\mu = \nu_m$.*

Remark 3.3.3 The above lemma is just a special case of the Pieri formula, which was conjectured to hold for a more general insertion algorithm in [1] and was later proved by other methods by Bergeron and Sotille in [2].

Lemma 3.3.4 *The polynomials S_{ν_m} generate the ring of symmetric polynomials in n variables. That is each symmetric polynomial S can be written as*

$$S = \sum_{(m_1,\ldots,m_k)\in M_+} S_{\nu_{m_1}} \cdots S_{\nu_{m_k}} - \sum_{(m'_1,\ldots,m'_k)\in M_-} S_{\nu_{m'_1}} \cdots S_{\nu_{m'_k}} \tag{3.4}$$

where M_+ and M_- are two sets of sequences of positive numbers.

Lemma 3.3.5 *Let R be an RC-graph then*

$$R \leftarrow yxz = R \leftarrow yzx \quad \textit{if} \quad 0 < x < y \leq z \leq n$$

and

$$R \leftarrow xzy = R \leftarrow zxy \quad \textit{if} \quad 0 < x \leq y < z \leq n.$$

Corollary 3.3.6 *If R is an RC-graph and Y_1 and Y_2 are two Young tableaux then*

$$R \leftarrow (Y_1 \leftarrow Y_2) = (R \leftarrow Y_1) \leftarrow Y_2.$$

We postpone the proofs of the above three lemmas until the next Section. Let us just note that Corollary 3.3.6 follows easily from Lemma 3.3.5 and Fact (3.1).

Let us show how Theorem 3.3.1 can be proved using the above three lemmas. We define the sets $\mathcal{R}_w$ and $\mathcal{Y}_\mu$ to be

$$\mathcal{R}_w = \bigcup_{w_R = w} R \text{ and } \mathcal{Y}_\mu = \bigcup_{\mu(Y)=\mu} Y.$$

If

$$\mathcal{R} = \mathcal{R}_w \cdot \mathcal{Y}_\mu = \bigcup_{R \in \mathcal{R}_w, Y \in \mathcal{Y}_\mu} R \leftarrow Y,$$

we would like to show that

$$\mathcal{R} = \bigcup_u \mathcal{R}_u. \tag{3.5}$$

This implies that each $\mathcal{R}_u$ is taken $c^u_{w,\mu}$ times in the above union, since there is a unique way of writing $S_w S_\mu$ as a sum of Schubert polynomials. Hence (3.5) will prove the theorem.

Use Lemma 3.3.4 to write

$$S_\mu = \sum_{(m_1,\ldots,m_k) \in M_+} S_{\nu_{m_1}} \cdots S_{\nu_{m_k}} - \sum_{(m_1,\ldots,m_k) \in M_-} S_{\nu_{m_1}} \cdots S_{\nu_{m_k}}$$

this immediately implies that

$$\mathcal{Y}_\mu = \bigcup_{(m_1,\ldots,m_k) \in M_+} \mathcal{Y}_{\nu_{m_1}} \cdots \mathcal{Y}_{\nu_{m_k}} - \bigcup_{(m_1,\ldots,m_k) \in M_-} \mathcal{Y}_{\nu_{m_1}} \cdots \mathcal{Y}_{\nu_{m_k}} \tag{3.6}$$

where the minus stands for the set theoretic difference of the two sets and where $\mathcal{Y}_{\mu_1} \cdot \mathcal{Y}_{\mu_2} = \bigcup_{\mu(Y_1)=\mu_1, \mu(Y_2)=\mu_2} Y_1 \leftarrow Y_2$.

The reason why we can take the set theoretic difference in the above formula is the following. By Lemma 3.3.2 both first and second sets in (3.6) could be broken up into unions of $\mathcal{Y}_{\mu'}$ (since any insertion into a Young tableaux produces a Young tableaux). But since S_μ cannot be written as a nontrivial linear expression of $S_{\mu'}$'s the set theoretical difference above is well defined.

Thus we can conclude:

$$\mathcal{R} = \mathcal{R}_w \cdot (\bigcup_{(m_1,\ldots,m_k)\in M_+} \mathcal{Y}_{\nu_{m_1}} \cdots \mathcal{Y}_{\nu_{m_k}}) - \mathcal{R}_w \cdot (\bigcup_{(m_1,\ldots,m_k)\in M_-} \mathcal{Y}_{\nu_{m_1}} \cdots \mathcal{Y}_{\nu_{m_k}})$$

Using Corollary 3.3.6 we can immediately see that the set theoretic difference is well-defined in the above formula. On the other hand, this formula and Lemma 3.3.2 shows that $\mathcal{R}$ can be written in the form (3.5), since by Lemma 3.3.2 each $\mathcal{R}_w \cdot \mathcal{Y}_{\nu_{m_1}} \cdots \mathcal{Y}_{\nu_{m_k}}$ is a union $\bigcup_u \mathcal{R}_u$. This finishes the proof of the Theorem 3.3.1.

3.4 Technical details in the proof of Littlewood-Richardson rule.

Proof. (of Lemma 3.3.2) The proof of this Lemma will just be a combination of Monk's rule and Lemma 3.2.2. We have already mentioned that a more general case of this Lemma was conjectured in [1], but no proof was provided there, since Lemma 3.2.2 does not hold for the general algorithm.

Let $Y = (1 \leq a_1 \leq a_2 \leq \ldots \leq a_m \leq n)$ be a filling of the Young diagram ν_m. We can easily see from the insertion algorithm that

$$w_{R\leftarrow Y} = w_{R\leftarrow a_1\ldots a_m} = s_{c_m,d_m}\ldots s_{c_1,d_1} w_R$$

where $c_i > 0 \geq d_i$, $d_1 > d_2 > \ldots > d_m$ and $l(s_{c_m,d_m}\ldots s_{c_1,d_1} w_R) = l(w_R) + m$.

Conversely, assume we are given an RC-graph R' with $w_{R'} = s_{c_m,d_m}\ldots s_{c_1,d_1} w_R$ with $c_i > 0 \geq d_i$, $d_1 > d_2 > \ldots > d_m$ and $l(s_{c_m,d_m}\ldots s_{c_1,d_1} w_R) = l(w_R) + m$. Then we can go through the inverse insertion algorithm and delete one by one intersections of strands c_i

and d_i. We will get m numbers $a_1, ..., a_m$.

Moreover, by Lemma 3.2.2, $a_i \leq a_{i+1}$ (otherwise we would not have $d_i < d_{i+1}$). Thus we have even proved a slightly better version of the Lemma:

$$S_w S_{\nu_m} = \sum S_{s_{c_m,d_m} \cdots s_{c_1,d_1} w}$$

where $c_i > 0 \geq d_i$, $d_1 > d_2 > ... > d_m$ and $l(s_{c_m,d_m} ... s_{c_1,d_1} w_R) = l(w_R) + m$. □

Proof. (of Lemma 3.3.4) Let us define a lexicographical ordering on Young diagrams. We say that $\mu = (\mu_1, ..., \mu_k) > \tilde{\mu} = (\tilde{\mu}_1, ..., \tilde{\mu}_{\tilde{k}})$ if either $k > \tilde{k}$ or $k = \tilde{k}$, $\mu_k = \tilde{\mu}_k$, ..., $\mu_{i+1} = \tilde{\mu}_{i+1}$, but $\mu_i > \tilde{\mu}_i$ for some i.

We will prove that every Schur polynomial S_μ can be written in the form (3.4) by induction. As the base of the induction, we use the case $k = 1$, then μ is just ν_m and there is nothing to prove.

Let's assume that we can prove (3.4) for every $\tilde{\mu}$, which is smaller than $\mu = (\mu_1, ..., \mu_k)$. Let $\mu' = (\mu_1, ..., \mu_{k-1})$ be the partition with the last row of μ deleted. The product $S_{\tilde{\mu}} S_{\nu_{\mu_k}}$ can be written as a sum of Schur polynomials by Lemma 3.3.2 and since insertion into a Young tableaux produces a Young tableaux. Moreover, each of those Schur polynomials will correspond to a Young diagram, which is less than or equal to μ. This can be easily deduced by looking at how insertion algorithm works: an insertion into a Young tableau adds exactly one box to the corresponding Young diagram. So

$$S_{\tilde{\mu}} S_{\nu_{\mu_k}} = \sum_{\mu'} c^{\mu'}_{\mu,\nu_{\mu_k}} S_{\mu'} \tag{3.7}$$

where every μ' is smaller than or equal to μ with respect to the lexicographical ordering.

To finish the proof we will show that $c^{\mu}_{\mu,\nu_{\mu_k}} = 1$. If we fill the ith row of $\tilde{\mu}$ with $i+1$, and we fill ν_m with ones, then the result Y_0 of the insertion will have the shape of μ. On the other hand, this is a unique way of getting Young tableaux Y_0 using this kind of insertion. So $c^{\mu}_{\mu,\nu_{\mu_k}} = 1$. Hence using (3.7) we can express S_μ as a sum of products of Schur polynomials $S_{\mu'}$, such that each μ' is smaller than μ. Thus by induction assumption S_μ can be written in the form (3.4). □

The rest of this Section will be concerned with the proof of Lemma 3.3.5.

Recall that the first part of Lemma 3.3.5 followed from Lemma 3.2.2. So, we just have

to prove the second part of it:

$$R \leftarrow xzy = R \leftarrow zxy \quad \text{for any } R \text{ and } 0 < x \leq y < z \leq n \tag{3.8}$$

The path of x in $R \leftarrow xz$ is weakly to the left of the path of z. If it is strictly to the left of the path of z (in other words the right path $r(x)$ of x has no common parts with the left path $\ell(z)$), then clearly $R \leftarrow xz = R \leftarrow zx$ and (3.8) holds. An example for this situation would be $x = 1$, $y = 2$, $z = 3$ and $R = R_3$ (the third RC-graph from Figure 9).

Hence we just have to look at the case when right path of x partially coincides with the left path of z. Let's assume that the top row where this happens is k. Then by above argument, $R \leftarrow xzy = R \leftarrow zxy$ for all rows, which are above the row k.

Assume that during the insertion of x into R an intersection $(i_j(x), k_j(x))$ was inserted into R, such that $k_j(x) < k$ but $k_{j+1}(x) > k$. Denote by s_1 and s_2 the two pieces of strands, which connect $(i_j(x), k_j(x))$ with $(\ell_{j+1}(x), k_{j+1}(x))$. Set $a = a_j(x) > 0 \geq b = b_j(x)$. So that during the insertion of x into R, the labeling of s_1 changed from a to b, while the labeling of s_2 changed from b to a.

Assume that during the insertion of z into $R \leftarrow x$ we insert an intersection of strands at the place $(i, k) = (i_{j'}(z), k_{j'}(z))$. Then we know that one of the strands at (i, k) is s_2. Denote by s_2' the piece of this strand, which connects (i, k) with $(\ell_{j'+1}(z), k_{j'+1}(z))$. ($s_2$ and s_2' have a common piece between the rows k and $k_{j+1}(x)$.) Take the other strand coming out of (i, k) and denote the piece of this strand, which connects (i, k) with $(i_{j'+1}(z), k_{j'+1}(z))$, by s_3. Clearly, $a_{j'}(z) = a$ and we set $b_{j'}(z) = c$.

Since the paths of y have to sit between the right path of x and the left path of z above row k, the strand s_2 has to become a part of the left path of the insertion of y into $R \leftarrow xz$. Assume it happened at some place $(i_1, k_1) = (i_{j''}(y), k_{j''}(y))$. We claim that $(i, k) = (\ell_{j''+1}(y), k_{j''+1}(y))$. In other words, the strands, which pass through (i_1, k_1) in R have to pass through (i, k) in R. If this claim does not hold, then the strand labeled by $c \leq 0$ has to pass between the left and right paths of y, which is impossible. Denote by s_3' the right path, which connects (i_1, k_1) with (i, k), so that s_3' and s_3 are two pieces of the same strand in R.

Thus during the insertion algorithm of y into $R \leftarrow xz$ we had to remove intersection (i, k) and find an open space to the left of it, call it $(\bar{i}, k) = (i_{j''+1}(y), k_{j''+1}(y))$.

We have two cases:

Case 1. $(\bar{i}, k)$ is to the left of the strand s_1.

Case 2. $(\bar{i}, k)$ is to the right of the strand s_1.

Before going through the proofs for both cases, let us give two examples. Case 1 happens when we take $x = y = 2$, $z = 3$ and $R = R_3$ from Figure 9. For Case 2 take $n = 2$ and $R = \{(2, 2)\}$ then $x = y = 1$ and $z = 2$ will produce Case 2.

Proof of Case 1. First of all let us note that $(\bar{i}, k)$ is to the left of s_1 if and only if the stand s_1 passes exactly to the left of strand s_2 in the row k, that is there are no other strands between s_1 and s_2 in the row k. Indeed, if we had other strands between them they had to be positive in R (since they lie between right and left paths of x), but then $(i-1, k)$ would be an open space, so that $\bar{i} = i - 1$, which contradicts the fact that $(\bar{i}, k)$ is to the left of the strand s_1. This argument also proves that $(\bar{i}, k)$ is to the right of s_1 if and only if $\bar{i} = i - 1$, which will be used in the proof of the second case.

Denote by p_1^x the path of the insertion of x into R below the row k, by p_1^z the path of the insertion of z into $R \leftarrow x$ below the row k and by p_1^y the path of the insertion of y into $R \leftarrow xz$ below the row k. Notice that since $(\bar{i}, k)$ is to the left of s_1 we can conclude that p_1^z is weakly to the right of p_1^x, while p_1^y is weakly to the left of p_1^x.

Let us think how $R \leftarrow zxy$ looks in this case. When we insert z into R, the open space $(i_{j'}(z), k_{j'}(z))$ in the row k is no longer (i, k), but it is now $(i-1, k)$. Indeed, s_1 is labeled by $a > 0$ while s_2 is labeled by $b \leq 0$ in R, moreover, s_1 passes through the space $(i-1, k)$ and together with s_2 creates an open space. So we insert $(i-1, k)$ into R and denote by p_2^z the path of z in R below the row k. Notice that the paths p_2^z and p_1^x are identical. When we insert x into $R \leftarrow z$, at the row k we have to remove $(i-1, k) = (\ell_{j+1}(x), k_{j+1}(x))$, since s_1 and s_2 intersect at $(i-1, k)$ in $R \leftarrow z$. So, we remove $(i-1, k)$ and insert $(\bar{i}, k) = (i_{j+1}(x), k_{j+1}(x))$ into $R \leftarrow z$. Denote by p_2^x the path of x in $R \leftarrow z$ below row k. Notice that p_2^x is identical with p_1^y. At the same time, the path p_2^y of the insertion of y into $R \leftarrow zx$ below the row k will be identical with p_1^z.

To summarize, we have $R \leftarrow xzy = R \leftarrow zxy$ above the row k. Below the row k we first insert into R along the path $p_2^z = p_1^x$ in both cases. Then we insert along p_1^z and along p_1^y for $R \leftarrow xzy$ and along p_2^x and along p_2^y for $R \leftarrow xzy$. But since $p_1^z = p_2^y$ is weakly to the right of $p_2^z = p_1^x$ while $p_2^x = p_1^y$ is weakly to the left of $p_2^z = p_1^x$, we can apply Lemma 3.2.2 to show that paths $p_1^z = p_2^y$ and $p_2^x = p_1^y$ are separated by $p_2^z = p_1^x$ and hence it does not

matter along which path below the row k we insert first. This proves $R \leftarrow xzy = R \leftarrow zxy$ below the row k and finishes the proof of Case 1.

Proof of Case 2. The situation in case 2 is just slightly more difficult than in Case 1.

Denote by $\tilde{k}$ the row where the path of the insertion of z into $R \leftarrow x$ moves to the left of s_1 (this has to happen below the row k, but above the row k_{j+1}). As in Case 1 in the row $\tilde{k}$ the strand s_1 has to pass directly to the left of s_2. And we can define paths p_i^x, p_i^y and p_i^z for $i = 1, 2$, which lie below the row $\tilde{k}$, the same way we have done it in the first case.

Then we can apply the same argument to these paths to show that $R \leftarrow xzy = R \leftarrow zxy$ below the row $\tilde{k}$ and above the row k. It is just left to check that $R \leftarrow xzy = R \leftarrow zxy$ between the rows k and $\tilde{k}$. But for $R \leftarrow xzy$ when we insert x or z no intersections are inserted between the rows k and $\tilde{k}$, denote by p the path of the insertion of y between the rows k and $\tilde{k}$. At the same time, nothing is inserted between the rows k and $\tilde{k}$ for $= R \leftarrow zxy$, when we insert x or y and the path for z between the rows k and $\tilde{k}$ is identical with p. This finishes the proof of Lemma 3.3.5 in the second case.

Appendix A

Equivariant Cohomology and Currents

Let G be a compact Lie group and M a compact oriented manifold equipped with a G action. Let $\Omega(M)$ be the space of smooth forms on M and $S(\mathfrak{g}^*)$ be the space of polynomials on the Lie algebra $\mathfrak{g}$. We define the differential d_G on $\Omega_G(M) = (\Omega(M) \otimes S(\mathfrak{g}^*))^G$ as follows. If $\xi \in \mathfrak{g}$ and X_ξ is the infinitesimal vector field on M generated by ξ, then for $\alpha \otimes f \in \Omega_G(M)$

$$d_G(\alpha \otimes f)(\xi) = d\alpha \otimes f(\xi) - i(X_\xi)\alpha \otimes f(\xi).$$

$\Omega_G(M)$ together with d_G produces a chain complex, which defines the equivariant cohomology $H_G(M)$ (for detailed exposition of the subject see [14]).

Let $\mathcal{E}(M)$ denote the space of currents on M. We will recall a few facts about currents. All the definitions and details can be found in [6]. A current T of degree k acts on forms of degree $\dim M - k$ (sometimes we say that this current also has dimension $\dim M - k$). Moreover, we can define the boundary operation ∂ which decreases the dimension of a current by one and satisfies

$$\partial T(\alpha) = (-1)^{\deg T} T(d\alpha)$$

for every form $\alpha \in \Omega_G(M)$.

∂ is called the boundary operator, since it has the following important property. Let $N \subset M$ be a smooth oriented compact submanifold with possibly nontrivial boundary ∂N.

Integrations over N and ∂N are then currents on M denoted by $\{N\}$ and $\{\partial N\}$ and

$$\partial\{N\} = \{\partial N\}.$$

If N has no boundary, it defines a cohomology class denoted by $[N]$. Moreover, if N has singularities of codimension at least 2, they do not change $\partial\{N\}$ or $[N]$.

We can also define the contraction operation by a vector field X as

$$i(X)T(\alpha) = (-1)^{\deg T} T(i(X)\alpha).$$

The equivariant cohomology $\mathcal{H}_G^*(M)$ is defined using $\mathcal{E}_G(M) = (\mathcal{E}(M) \otimes S(\mathfrak{g}^*))^G$ and the equivariant boundary operator ∂_G which is given by

$$\partial_G(T \otimes f)(\xi) = \partial T \otimes f(\xi) - i(X_\xi)T \otimes f(\xi)$$

for $T \otimes f \in \mathcal{E}_G(M)$.

Notice that if $N \subset M$ is an invariant oriented compact submanifold then $\{N\} = \{N\} \otimes 1 \in (\mathcal{E}(M) \otimes S(\mathfrak{g}^*))^G$. Moreover $i(X_\xi)\{N\} = 0$ for any $\xi \in \mathfrak{g}$. Hence

$$\partial_G\{N\} = \{\partial N\}.$$

and if ∂N is empty, N defines an equivariant cohomology class denoted by $[N]$ (again, singularities of codimension at least 2 do not change anything).

If $f : M \to N$ is an invariant map between two G-manifolds. Then we can define the pullback map $f^* : \Omega_G(N) \to \Omega_G(M)$. It descends to the pullback map on the equivariant cohomology $f^* : H_G(N) \to H_G(M)$, moreover, it is a ring homomorphism. We can also define by duality a pushforward map $f_* : \mathcal{E}_G^i(M) \to \mathcal{E}_G^{i+\dim N - \dim M}(N)$. This map defines $f_* : \mathcal{H}_G^i(M) \to \mathcal{H}_G^{i+\dim N - \dim M}(N)$, which is a $S(\mathfrak{g}^*)$-module homomorphism.

We will need one more definition. Let $\pi : M \to N$ be a smooth fibration with possibly noncompact fibers. Then we can define the pushforward map: $\pi_* : \Omega^i(M)_c \to \Omega^{i+\dim N - \dim M}(N)$ by integrating along the fibers (where c stands compactly supported forms). We can also define the pullback $\pi^* : \mathcal{E}^*(N) \to \mathcal{E}^*(M)_c$ by $\pi^* T(\alpha) = T(\pi_*(\alpha))$ for a compactly supported form α.

Theorem A.0.1 *$\mathcal{H}^*_G(M)$ is isomorphic to $H^*_G(M)$.*

Proof. We will construct a map $\rho : \mathcal{E}^*_G(M) \to \Omega^*_G(M)$ together with a homotopy operator $Q : \mathcal{E}^{*+1}_G(M) \to \Omega^*_G(M)$, which satisfies

$$\rho = Id + Q\partial_G + d_G Q.$$

This will be enough to prove the theorem.

It is well known that M can be invariantly embedded into $\mathbb{R}^n$ (see [20]), which is equipped with a linear G action. Let $i : M \to \mathbb{R}^n$ be this embedding. Let $U \subset \mathbb{R}^n$ be a small invariant tubular neighborhood of $i(M)$ with the projection $\pi : U \to M$. Choose a small invariant open ball B around the origin of $\mathbb{R}^n$, such that if $x \in i(M)$ and $b \in B$, then $x + i(b) \in U$.

Let p_1 and p_2 be the projections of $M \times B$ onto M and B respectively, and let $\kappa : M \times B \to U$ be the map $\kappa(x, b) = i(x) - b$. Let $\tau \in \Omega_G(B)$ be the compactly supported Mathai-Quillen form, which satisfies:

$$p_*\tau = 1 \text{ and } d_G\tau = 0$$

for the map $p : B \to$point. This form was explicitly constructed in [21] (for another exposition see [14]).

For $\mu \in \mathcal{E}_G(M)$, define

$$\rho(\mu) = (p_1)_*(\kappa^*\pi^*(\mu) \wedge p_2^*(\tau))$$

(note that both κ and π are fibrations, so $\kappa^*\pi^*$ is well-defined on currents.) Morally speaking, $\rho(\mu)$ is a convolution of μ and τ. So, it is easy to conclude that $\rho(\mu)$ is a smooth form on M.

$\pi\kappa$ is equivariantly homotopic to p_1 via $\pi(\kappa_t(x, b)) = \pi(i(x) - tb)$. So we can find $\tilde{Q} : \mathcal{E}^{*+1}(M) \to \mathcal{E}^*(M \times B)$ with

$$\kappa^*\pi^* - p_1^* = \tilde{Q}\partial_G + \partial_G\tilde{Q}.$$

(p_1^* is well-defined on currents, since it is also a smooth fibration.)

Thus

$$\begin{aligned}\rho(\mu) &= (p_1)_*(p_1^*\mu \wedge p_2^*\tau) + (p_1)_*((\tilde{Q}\partial_G\mu) \wedge p_2^*\tau + (\partial_G\tilde{Q}\mu) \wedge p_2^*\tau) \\ &= \mu + Q\partial_G\mu + d_G Q\mu\end{aligned}$$

where $Q\mu = (p_1)_*(\tilde{Q}\mu \wedge p_2^*\tau)$. Notice that we have used both properties of Mathai-Quillen form τ in the above equation. $\square$

Bibliography

[1] N. Bergeron, S. Billey. *RC-graphs and Schubert polynomials.* Experiment. Math. 2 (1993), no. 4, 257–269.

[2] N. Bergeron, F. Sotille. *A Pieri-type formula for isotropic flag manifolds.* MSRI Preprint 1998-050, arxiv:math.CO/9810025

[3] I. N. Bernšteĭn, I. M. Gelfand, S. I. Gelfand. *Schubert cells, and the cohomology of the spaces G/P.* (Russian) Uspehi Mat. Nauk 28 (1973), no. 3(171), 3–26

[4] S. Billey, W. Jockusch, R. Stanley. *Some combinatorial properties of Schubert polynomials.* J. Algebraic Combin. 2 (1993), no. 4, 345–374.

[5] C. Chevalley. *Sur les dcompositions cellulaires des espaces G/B.* With a foreword by Armand Borel. Proc. Sympos. Pure Math., 56, Part 1, Algebraic groups and their generalizations: classical methods (University Park, PA, 1991), 1–23, Amer. Math. Soc., Providence, RI, 1994.

[6] G. De Rham. *Differentiable manifolds. Forms, currents, harmonic forms.* Fundamental Principles of Mathematical Sciences, 266. Springer-Verlag, Berlin-New York, 1984.

[7] S. Fomin, A. Kirillov. *The Yang-Baxter equation, symmetric functions, and Schubert polynomials.* Proceedings of the 5th Conference on Formal Power Series and Algebraic Combinatorics (Florence, 1993). Discrete Math. 153 (1996), no. 1-3, 123–143.

[8] S. Fomin, R. Stanley. *Schubert polynomials and the nil-Coxeter algebra.* Adv. Math. 103 (1994), no. 2, 196–207.

[9] W. Fulton. *Young tableaux. With applications to representation theory and geometry.* London Mathematical Society Student Texts, 35. Cambridge University Press, Cambridge, 1997.

[10] I. M. Gelfand, M. L. Cetlin. *Finite-dimensional representations of the group of unimodular matrices.* Doklady Akad. Nauk SSSR (N.S.) 71, (1950). 825–828.

[11] R. Goldin. *The cohomology of weight varieties.* Ph.D. Theses, MIT, 1999.

[12] N. Gonciulea, V Lakshmibai. *Degenerations of flag and Schubert varieties to toric varieties.* Transform. Groups 1 (1996), no. 3, 215–248.

[13] V. Guillemin, S. Sternberg. *The Gelfand-Cetlin system and quantization of the complex flag manifolds.* J. Funct. Anal. 52 (1983), no. 1, 106–128.

[14] V. Guillemin, S. Sternberg. *Supersymmetry and equivariant de Rham theory.* Mathematics Past and Present. Springer-Verlag, Berlin, 1999.

[15] V. Guillemin, S. Sternberg. *Symplectic techniques in physics.* Second edition. Cambridge University Press, Cambridge, 1990.

[16] F. Kirwan. *Cohomology of quotients in symplectic and algebraic geometry.* Mathematical Notes, 31. Princeton University Press, Princeton, N.J., 1984.

[17] D. Knuth *Permutations, matrices, and generalized Young tableaux.* Pacific J. Math. 34 1970 709–727.

[18] V. Lakshmibai. *Kempf varieties.* J. Indian Math. Soc. (N.S.) 40 (1976), no. 1-4, 299–349 (1977).

[19] A. Lascoux, M.-P. Schutzenberger. *Polynomes de Schubert.* (French) [Schubert polynomials] C. R. Acad. Sci. Paris Sir. I Math. 294 (1982), no. 13, 447–450.

[20] I. G. Macdonald *Notes on Schubert Polynomials* Montreal, Canada : Departement de mathematiques et d'informatique, Universite du Quebec a Montreal, 1991

[21] V. Mathai, D. Quillen *Superconnections, Thom classes, and equivariant differential forms.* Topology 25 (1986), no. 1, 85–110.

[22] G.D. Mostow, *Equivariant embeddings in Euclidean space.* Ann. of Math. (2) 65 (1957), 432–446

[23] C. Schensted. *Longest increasing and decreasing subsequences.* Canad. J. Math. 13 1961 179–191.

[24] R. Winkel. *A combinatorial bijection between Standard Young Tableaux and reduced words of Grassmannian permutations.* Sem. Loth. Comb. B36h (1996).